



# Assessment of sediment physiochemical properties, microbial and predicted functional diversity in mangrove eco-restoration sites of Hamata, Mangrove Bay, and Saffaga along the Egyptian Red Sea coast

Muziri Mugwanya<sup>1</sup> · Eric Zadok Mpingirika<sup>1,2</sup> · Yasmine AbdelMaksoud<sup>1</sup> · Rafat A. Eissa<sup>1</sup> · Hani Sewilam<sup>1,3</sup>

Received: 8 April 2025 / Accepted: 15 November 2025  
© The Author(s) 2025

## Abstract

Microbial communities perform important roles in nutrient cycling, degradation of environmental pollutants, and support of various life forms on Earth. Mangroves live in very harsh environments, and if not for the existence of several microbial species in their ecosystems, they would not survive. The Egyptian Red Sea coast is dominated by two mangrove species, *Avicennia marina* and *Rhizophora mucronata*, which serve as breeding grounds for marine organisms and aid in carbon sequestration. Despite their ecological significance, comparative studies examining the physiochemical properties and heavy metal concentration of mangrove sediments of two dominant species along the Egyptian Red Sea coast (Hamata, Mangrove Bay, and Saffaga) and their relationship to microbial and functional diversity are scarce. Our findings revealed significant differences in sodium ions, potassium ions, organic carbon, and bulk density at 30–50 cm depth across the locations. Heavy metal analysis revealed significantly lower concentrations of zinc and manganese and high concentrations of copper in sediment samples collected from Mangrove Bay at all sampling depths. Metagenomics analysis revealed that the dominant phyla across the three sites were *Pseudomonadota*, *Bacillota*, and *Bacteroidota*, along with *Actinomycetota*, and *Chloroflexota*, and unclassified bacteria. Within the phylum *Bacillota*, several major classes were identified, including *Bacillota\_A\_368345*, *Bacillota\_I*, and *Bacillota\_C*. Functional prediction revealed a higher abundance of microbes involved in energy metabolism and carbon cycle, whereas a lower abundance of microbes involved in sulfur and nitrogen cycles was noted across the sites. In conclusion, the identification of different microbial communities in sediments collected along the Egyptian Red Sea coastal areas suggests the role of different mangrove species and human activities in recruiting unique microbial species involved in promoting their survival under different environmental factors.

**Keywords** Bacterial ecology · Blue carbon ecosystems · Carbon sequestration · Mangroves · Sustainability

Responsible Editor: V.V.S.S. Sarma

✉ Hani Sewilam  
sewilam@lfi.rwth-aachen.de

Muziri Mugwanya  
muziri@aucegypt.edu

Eric Zadok Mpingirika  
empingirika@unmc.edu; zadok@aucegypt.edu

Yasmine AbdelMaksoud  
ymaksoud@aucegypt.edu

Rafat A. Eissa  
raafat.abdulmajeed@aucegypt.edu

<sup>1</sup> Center for Applied Research On the Environment and Sustainability (CARES), School of Science and Engineering, The American University in Cairo, AUC Avenue, P.O. Box 74, New Cairo 11835, Egypt

<sup>2</sup> Eppley Institute for Research in Cancer and Allied Diseases, University of Nebraska Medical Center, Omaha, NE 68198, USA

<sup>3</sup> UNESCO Chair in Hydrological Changes and Water Resources Management, RWTH Aachen University, Aachen, Germany

## Introduction

Mangroves are one of the world's most productive ecosystems along the coastal part of the tropical and subtropical regions (Ghosh et al. 2022; Wainwright et al. 2023; Alghamdi et al. 2024). Their coverage is approximately 150,000 km<sup>2</sup> across 123 countries, and they play a vital role in the habitation of various aquatic organisms, food supply, protection and stabilization of coastal areas, and aid in the phytoremediation of contaminated soils (Hossain et al. 2022; Baskaran et al. 2023; Farshid et al. 2023; Dajam et al. 2024; Karmakar et al. 2025). Their uptake of carbon dioxide (CO<sub>2</sub>) is estimated to be four times higher than that of inland terrestrial plants, and their annual carbon sequestration may reach up to 25.5 million tons (Patil et al. 2012; Ahmed et al. 2022; Chatting et al. 2022; Baskaran et al. 2023). The efficient carbon sequestration characteristic of mangroves is attributed to their high productivity and slow rates of decomposition of organic matter (OM) (Kida and Fujitake 2020; Guo et al. 2024), thus attracting the attention of the scientific community, which is keen on nature-based solutions for reducing greenhouse gases in the atmosphere.

Interestingly, mangrove ecosystems are rich in different microbial species (i.e., marine, freshwater, and terrestrial microbes) performing several biogeochemical processes such as carbon, sulfur, and nitrogen cycling and degradation of several organic and xenobiotic substances (Li et al. 2021a; Sarker et al. 2021; Padhy et al. 2022; Wang et al. 2022a; Ghose et al. 2024; Kannan et al. 2024). Moreover, the soil or sediment physiochemical properties, such as salinity, pH, electroconductivity (EC), organic carbon (OC), bulk density (BD), and elements or heavy metals (HMs) influence the activity of these microorganisms and the survival of mangrove forests (Lai et al. 2022; Li et al. 2022b). Hence, it is imperative to study the correlation between the soil or sediment's physiochemical properties and microbial composition. The application of next-generation sequencing (NGS) technologies in studying microbial diversity and composition has generated useful information in the literature, where several cultured, uncultured, and novel microbial species have been identified and extensively studied (Alam et al. 2021; Park et al. 2021). This unbiased approach detects all the genomes present in a sample and has been widely used in environmental microbiology (Tan et al. 2015; Nafea et al. 2024). For instance, Hu et al. (2022) reported *Pseudomonadota*, *Chloroflexi*, *Bacillota*, and *Bathyarchaeota* as the dominant bacterial phyla found in soil samples of the mangroves in South China. Moreover, heavy metals such as chromium (Cr), zinc (Zn), copper (Cu), lead (Pb), and nickel (Ni) were the main factors influencing microbial

diversity. From the Indian mangrove surface water, Ghosh et al. (2022) found that the *Pseudomonadota*, *Bacillota*, *Actinobacteria*, *Bacteroidota*, and *Cyanobacteria* were the dominant bacterial phyla present with Cu, Ni, and arsenic (As) resistance genes found in comparable abundances across the studied sites. Functional annotations revealed metabolic activities such as amino acids, carbohydrates, phosphorus, and nitrogen metabolisms to be uniformly distributed across the studied sites. A study on the *Avicennia marina* ecosystem along the Saudi Arabian Red Sea coastline revealed *Pseudomonadota* as the dominant phylum with functional prediction, indicating diverse microbial roles in HM uptake and plant growth promotion (Alghamdi et al. 2024). Moreover, a novel bacterial species, such as *Salinicola rhizosphaerae* (strain MSSRFH1<sup>T</sup>) has been identified from the rhizosphere of *A. marina* (Raju et al. 2016).

Based on NGS's massive data generation, this study, therefore, employed Illumina NGS of the V3–V4 hypervariable region of the 16S rRNA to (i) elucidate the microbial composition and diversity of sediment samples collected around *Avicennia marina* and *Rhizophora mucronata* mangrove species at three coastal sites along the Egyptian Red Sea coast, (ii) correlate the microbial composition and diversity patterns with the detected heavy metals in sediment samples, and (iii) predict the function of the detected microbiota in heavy metal contaminated sites. This is the first comparative analysis linking sediment physiochemistry, heavy metal contamination, and microbial functional diversity in Egyptian Red Sea mangroves (*Avicennia marina* and *Rhizophora mucronata*), and the study results will provide new knowledge that will be helpful in mangrove ecosystem management, conservation, and restoration.

## Materials and methods

### Sample collection

From 16th–19th March 2023, sediment samples were collected from three different locations along the Egyptian Red Sea coastline: Hamata (24°18'33.3"N, 35°21'43.64"E), Mangrove Bay (25°52'4.92"N, 34°24'55.99"E), and Saffaga (26°36'55.74"N, 34°0'46.17"E). Samples were coded as follows: HA, for sediment samples collected from Hamata around the *Avicennia marina* species; HR, for sediment samples collected from Hamata around the *Rhizophora mucronata* species; MA, for sediment samples collected from Mangrove Bay around the *A. marina* species; SA, for sediment samples collected from Saffaga around the *A. marina* species; and SR, for sediment samples collected from Saffaga around the *R. mucronata* species. The mangrove forests

in these locations have been affected by different human activities, such as urbanization, agriculture, and tourism. Moreover, the mangrove site in Saffaga is near a mining port (Abu Tartour Port). As such, the Egyptian government has taken a keen interest in restoring mangroves in these sites. Figure 1 shows the geographical sites from which the sediment samples were collected. Sediment samples (3 replicates) were collected around two dominant mangrove species, *Avicennia marina* and *Rhizophora mucronata*, at different depths (0–15 cm, 15–30 cm, 30–50 cm, and 50–100 cm) using soil augers of different depths. A GPS land area measurement meter (model: Mingzhe, model number: BEIMQWE12670JK) was used to mark the sampling sites. A total of 60 samples (i.e., 24 from Hamata, 12 from Mangrove Bay, and 24 from Saffaga) were collected and put in labelled, sterilized plastic bags. These samples were immediately put on dry ice and kept frozen until further analysis.

### Sediment sample analysis

At each sampling location (Hamata, Mangrove Bay, and Saffaga), sediment samples were collected and sectioned into four depth intervals: (0–15 cm, 15–30 cm, 30–50 cm, and 50–100 cm). For each depth interval, the collected sediment was thoroughly homogenized to create a composite sample

representative of the specific depth at that location. From this composite sample, three subsamples (replicates) were taken for subsequent physiochemical analysis at the Soil and Water Research Institute of the Agricultural Research Center (ARC) in Giza, Egypt, and heavy metal analysis. Briefly, 2 g of the sediment sample per replicate was air-dried and sieved through a 10-mesh sieve with a 2 mm aperture size (USA Standard Sieve). The soil pH and electroconductivity (EC) were measured as previously described by Sewilam et al. (2023). Organic carbon was determined as described by Dookie et al. (2024) with slight modifications. Briefly, 2 g of the sediment sample was used for organic carbon estimation. Twenty milliliters of potassium dichromate was added to the sediment sample, and the mixture was stirred for 1 min, followed by the addition of 40 ml of concentrated sulfuric acid. The mixture was left to stand for 30 min, and 400 ml of distilled water was added. Three drops of phenolphthalein indicator were added, and the mixture was titrated with 0.5 M ferrous sulfate until color changes. Organic carbon was calculated based on the equation below.

$$\text{Organic carbon} = (\text{ml of blank} - \text{ml of determination}) \times 0.399$$

Sediment cations and anions were measured according to the methods described by Madeira et al. (2003). For the sediment bulk density, this was determined as previously



**Fig. 1** Map showing the geographical sites from which the sediment samples were collected along the Egyptian Red Sea coast

described by Doran and Mielke (1984). Furthermore, the concentration of different heavy metals was analyzed using inductively coupled plasma (ICP) spectrometry (model Ultima 2 JY Plasma) (Soltanpour 1991).

### DNA extraction and sequencing

Sediment samples were transported on dry ice to the laboratory and immediately stored under  $-20^{\circ}\text{C}$  until further analysis. Sediment samples from a 0 to 15 cm depth per replicate were homogenized under sterilized conditions. Then, 400 mg of the sediment sample was used for total genomic DNA extraction using the innuSPEED Soil DNA Kit 2.0 (LOT No. 004–23), following the manufacturer's instructions. DNA concentration was determined by using the NanoDrop™ One/One<sup>C</sup> Microvolume UV–Vis Spectrophotometer from Thermo Fisher Scientific. Purity and completeness were evaluated using 1% agarose gel electrophoresis.

The 16S rRNA genes were amplified using the specific primers for V3 and V4 hypervariable regions: 341 F (CCT AYGGRBGCASCAG) and 806R (GGACTCANNNGG TATCTAAT) (Wu et al. 2024). PCR was performed in a 30  $\mu\text{L}$  reaction with 15  $\mu\text{L}$  Master Mix (New England Biolabs, USA), 0.2  $\mu\text{M}$  each of forward and reverse primers and 10 ng of template DNA. The thermocycling conditions were as follows: pre-degeneration at  $98^{\circ}\text{C}$  for 1 min, 30 cycles of denaturation at  $98^{\circ}\text{C}$  for 10 s, annealing at  $50^{\circ}\text{C}$  for 30 s, and extension at  $72^{\circ}\text{C}$  for 30 s, followed by a final extension at  $72^{\circ}\text{C}$  for 5 min. Electrophoretic detection was performed on a 2% agarose gel. Samples with a bright main band between 400 and 450 bp were selected for subsequent experiments. PCR products were purified using a kit (Tiangen Biotech, China). The purified products were used to prepare the library. Sequencing libraries were generated using the TIANSeq Fast DNA Library Prep Kit (Tiangen Biotech, China). Library quality was assessed on a Qubit 2.0 fluorometer (Thermo Scientific) and an Agilent 2100 Bioanalyzer. Finally, the libraries were sequenced on the Illumina platform using a  $2 \times 250$  bp paired-end protocol.

### 16S rRNA data processing and analysis

We used the Qiime2 pipeline (v2024.10) to process raw data (Bolyen et al. 2019). VSEARCH was used for denoising, chimera filtering and clustering. The quality of the processed sequences is presented in Supplementary Fig. 1. Filtered sequences were clustered by 97% similarity into operational taxonomic units (OTUs) with cluster-features-open-reference parameters against Greengenes2 (v2024.9) (Rognes et al. 2016; McDonald et al. 2024). Taxonomic assignment for each clustered OTU was performed using the Naive Bayes classifier trained against the Greengenes2 database. We used the microeco R package (v1.5.0) to calculate alpha

and beta diversity and visualization. Functional prediction for the abundance of communities was carried out using FAPROTAX (Louca et al. 2016) and Tax4Fun2 (Wemheuer et al. 2020) databases. Raw sequence reads have been deposited in the Sequence Read Archive (SRA) of the National Center for Biotechnology Information (NCBI) under a BioProject accession identification number PRJNA1224588.

### Statistical analysis

All datasets on the sediment physiochemical properties were subjected to normality and equality of variances tests using QQ plots and Levene's test, respectively. One-way analysis of variance (ANOVA) was conducted to determine significant differences in the measured parameters at  $p < 0.05$ . The Duncan Multiple Range test (DMRT) was used as a post hoc test to detect differences in the sediment sample means. Visualization of results was performed in R statistical programming language (version 4.3.2).

## Results

### Physiochemical properties of sediment samples

Table 1 presents the results of the physiochemical properties of sediment samples collected at different depths. No significant differences in the pH, electroconductivity (EC), sulfate ions ( $\text{SO}_4^{2-}$ ), bicarbonate ions ( $\text{HCO}_3^-$ ), chloride ions ( $\text{Cl}^-$ ), sodium ions ( $\text{Na}^+$ ), potassium ions ( $\text{K}^+$ ), magnesium ions ( $\text{Mg}^{2+}$ ), calcium ions ( $\text{Ca}^{2+}$ ), organic carbon (OC), and bulk density (BD) were noted across the sediment samples collected at 0–15 cm, 15–30 cm, and 50–100 cm depths. However, MA significantly ( $p < 0.05$ ) recorded higher pH values (8.31) than other sediment samples. Likewise, HR significantly recorded ( $p < 0.05$ ) lower values for the EC (10.42 dS/m),  $\text{Na}^+$  (46.53 meq/L), and  $\text{Ca}^{2+}$  (30.50 meq/L) compared to SA and SR at 30–50 cm depth. The OC content was significantly ( $p < 0.05$ ) higher in HA (0.64%) and SR (0.74%) than in other sediment samples at 30–50 cm depth.

### Heavy metal concentrations in sediment samples

The concentration of different heavy metals was assessed, and the results are presented in Table 2. MA sediment samples showed significantly ( $p < 0.05$ ) higher concentrations of Cu across all sampling depths compared to all other sites. Conversely, the MA samples had significantly ( $p < 0.05$ ) the lowest Cd concentrations at the 30–50 cm depth. At the 0–15 cm depth, MA (0.35 ppm) was significantly higher than all other sites (0.04–0.05 ppm). For cobalt (Co), significantly lower concentrations were noted in MA sediment samples at 0–15 cm, 30–50 cm, and 50–100 cm.

**Table 1** Physicochemical properties of sediment samples collected at different depths

Sample	pH (1:2.5)	EC (dS/m)	Anions (meq/L)			Cations (meq/L)			Ca <sup>2+</sup>	OC (%)	BD (g/cm <sup>3</sup> )
			SO <sub>4</sub> <sup>2-</sup>	HCO <sub>3</sub> <sup>-</sup>	Cl <sup>-</sup>	Na <sup>+</sup>	K <sup>+</sup>	Mg <sup>2+</sup>			
0–15 cm											
HA	8.17 <sup>a</sup> ±0.04	15.01 <sup>a</sup> ±1.50	67.15 <sup>a</sup> ±17.19	6.17 <sup>a</sup> ±1.15	94.5 <sup>a</sup> ±27.07	74.93 <sup>a</sup> ±20.98	1.88 <sup>a</sup> ±0.12	36.83 <sup>a</sup> ±10.69	54.17 <sup>a</sup> ±14.57	0.49 <sup>a</sup> ±0.04	1.31 <sup>a</sup> ±0.05
HR	8.26 <sup>a</sup> ±0.04	13.87 <sup>a</sup> ±1.91	55.28 <sup>a</sup> ±8.52	5.83 <sup>a</sup> ±0.58	77.50 <sup>a</sup> ±10.54	58.05 <sup>a</sup> ±4.68	1.90 <sup>a</sup> ±0.09	30.83 <sup>a</sup> ±5.69	47.50 <sup>a</sup> ±8.54	0.63 <sup>a</sup> ±0.24	1.31 <sup>a</sup> ±0.02
MA	8.33 <sup>a</sup> ±0.11	19.37 <sup>a</sup> ±3.48	82.62 <sup>a</sup> ±11.87	7.17 <sup>a</sup> ±0.58	101.83 <sup>a</sup> ±21.94	74.02 <sup>a</sup> ±6.61	2.63 <sup>a</sup> ±0.58	49.83 <sup>a</sup> ±17.21	65.83 <sup>a</sup> ±11.50	0.39 <sup>a</sup> ±0.20	1.46 <sup>a</sup> ±0.09
SA	8.23 <sup>a</sup> ±0.04	18.47 <sup>a</sup> ±4.36	75.01 <sup>a</sup> ±14.08	6.50 <sup>a</sup> ±1.00	100.50 <sup>a</sup> ±27.84	77.55 <sup>a</sup> ±18.28	1.80 <sup>a</sup> ±0.61	42.83 <sup>a</sup> ±10.50	62.50 <sup>a</sup> ±14.73	0.23 <sup>a</sup> ±0.16	1.34 <sup>a</sup> ±0.08
SR	8.03 <sup>a</sup> ±0.26	19.05 <sup>a</sup> ±3.13	70.45 <sup>a</sup> ±9.01	6.83 <sup>a</sup> ±1.15	113.17 <sup>a</sup> ±21.36	81.65 <sup>a</sup> ±17.86	1.50 <sup>a</sup> ±0.43	45.83 <sup>a</sup> ±7.37	61.50 <sup>a</sup> ±6.93	0.56 <sup>a</sup> ±0.06	1.34 <sup>a</sup> ±0.08
15–30 cm											
HA	8.17 <sup>a</sup> ±0.04	15.01 <sup>a</sup> ±1.50	67.15 <sup>a</sup> ±17.19	6.17 <sup>a</sup> ±1.15	94.5 <sup>a</sup> ±27.07	74.93 <sup>a</sup> ±20.98	1.88 <sup>a</sup> ±0.12	36.83 <sup>a</sup> ±10.69	54.17 <sup>a</sup> ±14.57	0.49 <sup>a</sup> ±0.04	1.31 <sup>a</sup> ±0.05
HR	8.26 <sup>a</sup> ±0.04	13.87 <sup>a</sup> ±1.91	55.28 <sup>a</sup> ±8.52	5.83 <sup>a</sup> ±0.58	77.50 <sup>a</sup> ±10.54	58.05 <sup>a</sup> ±4.68	1.90 <sup>a</sup> ±0.09	30.83 <sup>a</sup> ±5.69	47.50 <sup>a</sup> ±8.54	0.63 <sup>a</sup> ±0.24	1.31 <sup>a</sup> ±0.02
MA	8.33 <sup>a</sup> ±0.11	19.37 <sup>a</sup> ±3.48	82.62 <sup>a</sup> ±11.87	7.17 <sup>a</sup> ±0.58	101.83 <sup>a</sup> ±21.94	74.02 <sup>a</sup> ±6.61	2.63 <sup>a</sup> ±0.58	49.83 <sup>a</sup> ±17.21	65.83 <sup>a</sup> ±11.50	0.39 <sup>a</sup> ±0.20	1.46 <sup>a</sup> ±0.09
SA	8.23 <sup>a</sup> ±0.04	18.47 <sup>a</sup> ±4.36	75.01 <sup>a</sup> ±14.08	6.50 <sup>a</sup> ±1.00	100.50 <sup>a</sup> ±27.84	77.55 <sup>a</sup> ±18.28	1.80 <sup>a</sup> ±0.61	42.83 <sup>a</sup> ±10.50	62.50 <sup>a</sup> ±14.73	0.23 <sup>a</sup> ±0.16	1.34 <sup>a</sup> ±0.08
SR	8.03 <sup>a</sup> ±0.26	19.05 <sup>a</sup> ±3.13	70.45 <sup>a</sup> ±9.01	6.83 <sup>a</sup> ±1.15	113.17 <sup>a</sup> ±21.36	81.65 <sup>a</sup> ±17.86	1.50 <sup>a</sup> ±0.43	45.83 <sup>a</sup> ±7.37	61.50 <sup>a</sup> ±6.93	0.56 <sup>a</sup> ±0.06	1.34 <sup>a</sup> ±0.08
30–50 cm											
HA	8.16 <sup>b</sup> ±0.06	14.74 <sup>ab</sup> ±3.27	71.41 <sup>a</sup> ±13.97	7.17 <sup>a</sup> ±1.15	86.50 <sup>a</sup> ±15.87	68.38 <sup>bc</sup> ±9.63	2.73 <sup>ab</sup> ±0.48	39.50 <sup>a</sup> ±7.21	54.50 <sup>ab</sup> ±13.08	0.64 <sup>a</sup> ±0.16	1.30 <sup>b</sup> ±0.04
HR	8.16 <sup>b</sup> ±0.05	10.42 <sup>b</sup> ±2.04	41.52 <sup>a</sup> ±12.52	5.50 <sup>a</sup> ±1.73	65.83 <sup>a</sup> ±20.98	46.53 <sup>c</sup> ±12.89	1.98 <sup>bc</sup> ±0.54	27.17 <sup>a</sup> ±10.26	30.50 <sup>b</sup> ±1.00	0.37 <sup>b</sup> ±0.08	1.29 <sup>b</sup> ±0.23
MA	8.31 <sup>a</sup> ±0.08	18.62 <sup>ab</sup> ±3.73	74.78 <sup>a</sup> ±16.99	7.50 <sup>a</sup> ±0.00	103.88 <sup>a</sup> ±23.09	76.75 <sup>ab</sup> ±16.15	3.02 <sup>a</sup> ±0.29	43.50 <sup>a</sup> ±7.81	52.83 <sup>ab</sup> ±8.50	0.31 <sup>b</sup> ±0.00	1.48 <sup>a</sup> ±0.11
SA	8.17 <sup>b</sup> ±0.06	22.53 <sup>a</sup> ±1.15	83.95 <sup>a</sup> ±2.65	7.50 <sup>a</sup> ±0.00	131.83 <sup>a</sup> ±9.07	95.97 <sup>a</sup> ±5.09	1.32 <sup>c</sup> ±0.06	53.50 <sup>a</sup> ±1.00	74.50 <sup>a</sup> ±5.57	0.20 <sup>b</sup> ±0.06	1.40 <sup>ab</sup> ±0.02
SR	8.14 <sup>b</sup> ±0.06	20.44 <sup>a</sup> ±8.13	77.53 <sup>a</sup> ±28.72	7.50 <sup>a</sup> ±1.32	127.67 <sup>a</sup> ±56.87	85.63 <sup>ab</sup> ±19.97	2.25 <sup>ab</sup> ±0.52	48.83 <sup>a</sup> ±26.54	68.83 <sup>a</sup> ±24.95	0.74 <sup>a</sup> ±0.19	1.30 <sup>b</sup> ±0.08
50–100 cm											
HA	8.20 <sup>a</sup> ±0.11	20.83 <sup>a</sup> ±1.93	71.70 <sup>a</sup> ±22.31	6.50±1.00	96.50 <sup>a</sup> ±30.51	66.95 <sup>a</sup> ±12.65	1.73 <sup>a</sup> ±0.55	39.50 <sup>a</sup> ±13.75	57.50 <sup>a</sup> ±16.52	0.32 <sup>a</sup> ±0.22	1.28 <sup>a</sup> ±0.00
HR	8.22 <sup>a</sup> ±0.04	13.85 <sup>a</sup> ±5.79	51.82 <sup>a</sup> ±19.45	5.83±1.53	80.83 <sup>a</sup> ±37.21	61.23 <sup>a</sup> ±24.72	1.92 <sup>a</sup> ±0.29	31.50 <sup>a</sup> ±15.87	43.50 <sup>a</sup> ±18.33	0.29 <sup>a</sup> ±0.14	1.32 <sup>a</sup> ±0.06
MA	8.30 <sup>a</sup> ±0.10	18.84 <sup>a</sup> ±2.69	82.35 <sup>a</sup> ±14.38	7.50±1.00	98.50 <sup>a</sup> ±12.53	77.70 <sup>a</sup> ±10.61	2.65 <sup>a</sup> ±0.65	46.50 <sup>a</sup> ±7.21	61.50 <sup>a</sup> ±9.64	0.43 <sup>a</sup> ±0.00	1.45 <sup>a</sup> ±0.13
SA	8.20 <sup>a</sup> ±0.07	21.16 <sup>a</sup> ±3.98	87.88 <sup>a</sup> ±23.21	7.50±1.00	116.67 <sup>a</sup> ±21.83	86.77 <sup>a</sup> ±15.41	1.78 <sup>a</sup> ±0.32	54.17 <sup>a</sup> ±12.66	68.83 <sup>a</sup> ±11.93	0.27 <sup>a</sup> ±0.13	1.41 <sup>a</sup> ±0.05
SR	8.21 <sup>a</sup> ±0.04	17.11 <sup>a</sup> ±2.67	69.72 <sup>a</sup> ±10.86	9.50±1.00	94.50 <sup>a</sup> ±19.32	74.28 <sup>a</sup> ±14.84	2.24 <sup>a</sup> ±1.11	38.17 <sup>a</sup> ±5.13	56.17 <sup>a</sup> ±7.77	0.47 <sup>a</sup> ±0.15	1.39 <sup>a</sup> ±0.01

Tabular data is presented as mean ± SD. Different lower superscript letters in each column indicate significant differences at  $p < 0.05$ . EC electro conductivity,  $SO_4^{2-}$  sulfate ions,  $HCO_3^-$  hydrogen carbonate ions,  $Cl^-$  chloride ions,  $Na^+$  sodium ions,  $K^+$  potassium ions,  $Mg^{2+}$  magnesium ions,  $Ca^{2+}$  calcium ions, OC soil organic carbon, BD bulk density. Location and mangrove species: HA (Hamata, *Avicennia marina*), HR (Hamata, *Rhizophora mucronata*), MA (Mangrove Bay, *Avicennia marina*), SA (Saffaga, *Avicennia marina*), SR (Saffaga, *Rhizophora mucronata*)



**Table 2** The concentration of heavy metals in different sediment samples at different depths

Sample	Cu (ppm)	Cd (ppm)	Co (ppm)	Pb (ppm)	Fe (ppm)	Mn (ppm)	Zn (ppm)
0–15 cm							
HA	0.05 <sup>b</sup> ± 0.01	0.05 <sup>b</sup> ± 0.01	1.87 <sup>b</sup> ± 0.35	1.20 <sup>a</sup> ± 0.10	9.27 <sup>a</sup> ± 0.58	1.44 <sup>a</sup> ± 0.04	0.73 <sup>a</sup> ± 0.27
HR	0.04 <sup>b</sup> ± 0.01	0.04 <sup>b</sup> ± 0.01	1.13 <sup>c</sup> ± 0.06	0.57 <sup>a</sup> ± 0.32	9.26 <sup>a</sup> ± 1.41	1.48 <sup>a</sup> ± 0.07	0.59 <sup>ab</sup> ± 0.14
MA	0.35 <sup>a</sup> ± 0.05	0.35 <sup>a</sup> ± 0.05	2.25 <sup>b</sup> ± 0.08	0.53 <sup>a</sup> ± 0.14	7.03 <sup>b</sup> ± 0.70	1.22 <sup>a</sup> ± 0.34	0.34 <sup>b</sup> ± 0.01
SA	0.05 <sup>b</sup> ± 0.01	0.05 <sup>b</sup> ± 0.01	3.20 <sup>a</sup> ± 0.62	4.33 <sup>a</sup> ± 2.81	10.00 <sup>a</sup> ± 0.94	1.43 <sup>a</sup> ± 0.08	0.81 <sup>a</sup> ± 0.04
SR	0.05 <sup>b</sup> ± 0.01	0.05 <sup>b</sup> ± 0.01	3.67 <sup>a</sup> ± 0.21	3.27 <sup>a</sup> ± 2.25	9.43 <sup>a</sup> ± 0.74	1.40 <sup>a</sup> ± 0.35	0.79 <sup>a</sup> ± 0.12
15–30 cm							
HA	0.04 <sup>b</sup> ± 0.01	0.04 <sup>b</sup> ± 0.01	2.03 <sup>b</sup> ± 1.50	3.30 <sup>a</sup> ± 2.91	8.82 <sup>a</sup> ± 0.54	1.50 <sup>a</sup> ± 0.02	0.61 <sup>b</sup> ± 0.15
HR	0.04 <sup>b</sup> ± 0.01	0.04 <sup>b</sup> ± 0.01	1.53 <sup>b</sup> ± 0.65	3.37 <sup>a</sup> ± 3.42	9.87 <sup>a</sup> ± 0.18	1.54 <sup>a</sup> ± 0.12	0.62 <sup>ab</sup> ± 0.03
MA	0.33 <sup>a</sup> ± 0.10	0.33 <sup>a</sup> ± 0.10	2.26 <sup>b</sup> ± 0.08	0.44 <sup>a</sup> ± 0.28	7.58 <sup>a</sup> ± 1.51	1.04 <sup>b</sup> ± 0.36	0.40 <sup>c</sup> ± 0.03
SA	0.04 <sup>b</sup> ± 0.01	0.04 <sup>b</sup> ± 0.01	2.37 <sup>b</sup> ± 0.35	2.37 <sup>a</sup> ± 1.85	10.25 <sup>a</sup> ± 1.19	1.49 <sup>a</sup> ± 0.13	0.76 <sup>a</sup> ± 0.02
SR	0.05 <sup>b</sup> ± 0.01	0.05 <sup>b</sup> ± 0.01	3.93 <sup>a</sup> ± 0.42	1.27 <sup>a</sup> ± 0.64	9.63 <sup>a</sup> ± 1.36	1.54 <sup>a</sup> ± 0.07	0.74 <sup>ab</sup> ± 0.08
30–50 cm							
HA	0.05 <sup>b</sup> ± 0.01	0.63 <sup>a</sup> ± 0.25	2.17 <sup>b</sup> ± 0.81	1.30 <sup>a</sup> ± 0.69	10.08 <sup>a</sup> ± 0.92	1.39 <sup>a</sup> ± 0.24	0.69 <sup>ab</sup> ± 0.07
HR	0.06 <sup>b</sup> ± 0.01	0.80 <sup>a</sup> ± 0.61	1.17 <sup>c</sup> ± 0.31	2.70 <sup>a</sup> ± 2.86	9.60 <sup>a</sup> ± 0.59	1.39 <sup>a</sup> ± 0.18	0.59 <sup>b</sup> ± 0.05
MA	0.35 <sup>a</sup> ± 0.03	0.01 <sup>b</sup> ± 0.00	2.32 <sup>b</sup> ± 0.09	0.51 <sup>a</sup> ± 0.25	7.67 <sup>a</sup> ± 2.31	0.99 <sup>a</sup> ± 0.19	0.34 <sup>c</sup> ± 0.05
SA	0.06 <sup>b</sup> ± 0.01	0.50 <sup>ab</sup> ± 0.20	2.63 <sup>b</sup> ± 0.25	3.33 <sup>a</sup> ± 1.99	10.62 <sup>a</sup> ± 0.69	1.39 <sup>a</sup> ± 0.04	0.61 <sup>b</sup> ± 0.09
SR	0.04 <sup>b</sup> ± 0.01	0.90 <sup>a</sup> ± 0.20	4.13 <sup>a</sup> ± 0.40	0.70 <sup>a</sup> ± 0.53	9.45 <sup>a</sup> ± 0.61	1.39 <sup>a</sup> ± 0.11	0.75 <sup>a</sup> ± 0.04
50–100 cm							
HA	0.05 <sup>b</sup> ± 0.02	1.03 <sup>a</sup> ± 0.75	2.17 <sup>b</sup> ± 0.81	2.97 <sup>a</sup> ± 3.25	9.73 <sup>a</sup> ± 0.76	1.51 <sup>a</sup> ± 0.14	0.58 <sup>a</sup> ± 0.08
HR	0.05 <sup>b</sup> ± 0.01	0.40 <sup>a</sup> ± 0.10	1.17 <sup>c</sup> ± 0.31	0.84 <sup>a</sup> ± 0.75	9.75 <sup>a</sup> ± 0.95	1.37 <sup>a</sup> ± 0.11	0.53 <sup>a</sup> ± 0.18
MA	0.37 <sup>a</sup> ± 0.14	0.01 <sup>a</sup> ± 0.01	2.32 <sup>b</sup> ± 0.09	0.68 <sup>a</sup> ± 0.26	10.49 <sup>a</sup> ± 0.83	0.92 <sup>b</sup> ± 0.26	0.36 <sup>a</sup> ± 0.04
SA	0.04 <sup>b</sup> ± 0.00	0.60 <sup>a</sup> ± 0.10	2.63 <sup>b</sup> ± 0.25	3.00 <sup>a</sup> ± 2.25	10.78 <sup>a</sup> ± 0.83	1.49 <sup>a</sup> ± 0.19	0.63 <sup>a</sup> ± 0.12
SR	0.05 <sup>b</sup> ± 0.01	0.83 <sup>a</sup> ± 0.50	4.13 <sup>a</sup> ± 0.40	0.57 <sup>a</sup> ± 0.29	10.52 <sup>a</sup> ± 1.29	1.53 <sup>a</sup> ± 0.21	0.65 <sup>a</sup> ± 0.08

Tabular data is presented as mean ± SD. Different lower superscript letters in each column indicate significant differences at  $p < 0.05$ . Heavy metals: *Cu* copper, *Cd* cadmium, *Co* cobalt, *Pb* lead, *Fe* iron, *Mn* manganese, *Zn* zinc

No significant differences in the concentration of lead (Pb) and iron (Fe) were observed in all sediment samples across all depths except at 0–15 cm for Fe. For manganese (Mn), MA significantly ( $p < 0.05$ ) recorded the lowest concentrations at 15–30 cm and 50–100 cm depths compared to other sediment samples. Similarly, MA significantly ( $p < 0.05$ ) recorded the lowest values for zinc (Zn) at 15–30 cm and 30–50 cm depths compared to other sediment samples.

### Principal component analysis

The principal component analysis (PCA) was computed to elucidate the associations among the HMs to reveal that a considerable portion of the observed variability (65.3%) could be explained by the first two components (Fig. 2). Based on the PCA results, the contribution of the first and second axes to the HM's variance was found to be 46.6% and 18.7%, respectively. Moreover, the results indicate that iron (Fe) and manganese (Mn) are positively correlated and not correlated with zinc (Zn). Furthermore, copper (Cu) is negatively correlated with all the other HMs.

As indicated by the PCA biplots, there was an overlap of the biplots of Saffaga and Hamata, thus indicating similarities in the concentration of HMs in the sediments, unlike Mangrove Bay (Fig. 2a). Furthermore, there was an overlap of biplots for the two mangrove species, *A. marina* and *R. mucronata* (Fig. 2b), as well as an overlap of biplots for the different depths (Fig. 2c), which indicates similarities in HM concentrations in sediment samples obtained from such sources.

### Relative abundance, unique, and shared OTUs

The relative abundance of dominant bacteria at the phylum and class levels is shown in Fig. 3a and b, respectively. At the phylum level, *Pseudomonadota*, *Bacillota*, and *Bacteroidota* were dominant across the sites, though their proportions varied. In HA, *Bacillota* was most abundant, followed by *Bacteroidota* (17.9%) and *Pseudomonadota* (14.4%). In contrast, HR was dominated by unclassified bacteria (49.2%) and *Pseudomonadota* (24.9%). MA was heavily dominated by *Pseudomonadota* (67.6%), while SA showed a high

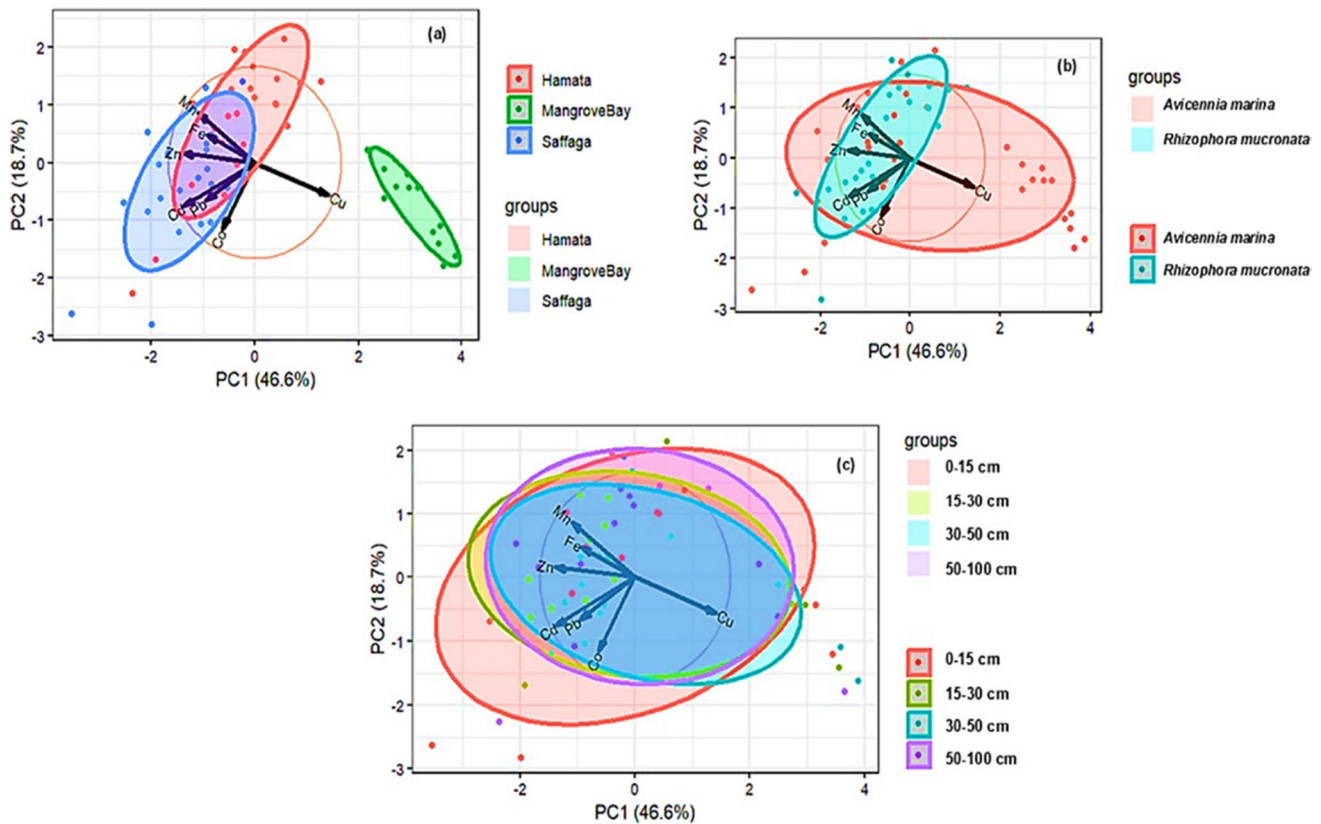


**Fig. 2** Principal component analysis (PCA) showing similarities and differences in heavy metal concentrations in sediment samples collected from **a** different locations, **b** mangrove species, and **c** depths

abundance of *Bacteroidota* (45.9%) and *Bacillota* (44.4%). SR was also dominated by *Pseudomonadota* (65.9%).

At the class level (Fig. 3b), *Clostridia* (37%), *Bacteroidia* (18%), *Bacilli* (13.3%), and *Gammaproteobacteria* (11.7%) were the dominant classes in HA sediment samples. In contrast, the unclassified bacteria (49.2%), *Gammaproteobacteria* (18.5%), *Dehalococcoidia* (7.9%), *Alphaproteobacteria* (6.4%), and *Bacilli\_A* (6.3%) were the dominant classes in HR sediment samples. For MA, the dominant classes were *Gammaproteobacteria* (48.9%), unclassified bacteria (23.3%), and *Alphaproteobacteria* (18.7%). SA sediment samples contained *Bacteroidia* (45.9%), *Clostridia\_258483* (28.1%), *Negativicutes* (11.6%), *Gammaproteobacteria* (6%), and *Bacilli* (4.7%) as the dominant classes. In contrast, *Gammaproteobacteria* (59.7%), *Bacilli* (10%), *Actinomycetes* (10%), *Clostridia* (5.2%), and *Alphaproteobacteria* (6.2%) were the dominant classes in SR sediment samples.

Figure 3c shows the unique and shared operational taxonomic units (OTUs) identified from sediment samples collected around *A. marina* and *R. mucronata* at different locations. Unique OTUs in HA were 261, 101 in HR, 31 in MA, 84 in SA, and 38 in SR. Only one OTU was shared among all the site locations and mangrove species. 11 OTUs were shared between HA and HR, 3 between HA and SR, 6

between HA and MA, 7 between HA and SA, 7 between HR and SR, 15 between HR and MA, 6 between HR and SA, 2 between SR and MA, 2 between SR and SA, 2 between SA and MA, 7 among HA, HR, and SR, 3 among HA, HR, and MA, and 3 among HR, SR, and MA.

### Alpha and beta diversity

The alpha and beta diversity indices are presented in Fig. 4a and b, respectively. Based on the data obtained concerning alpha diversity (Observed, ACE, and Simpson), no significant differences were noted between locations and mangrove species. Beta diversity indicated no clustering of the locations and mangrove species, thus indicating differences in the microbial composition between the locations and mangrove species. Moreover, PERMANOVA analysis indicated no significant differences in the locations' dissimilarity.

### Redundancy discrimination analysis

With a selection for the significant variables that influence microbial composition, we used the redundancy discrimination analysis (RDA) to depict the relationship between environmental variables and the composition of

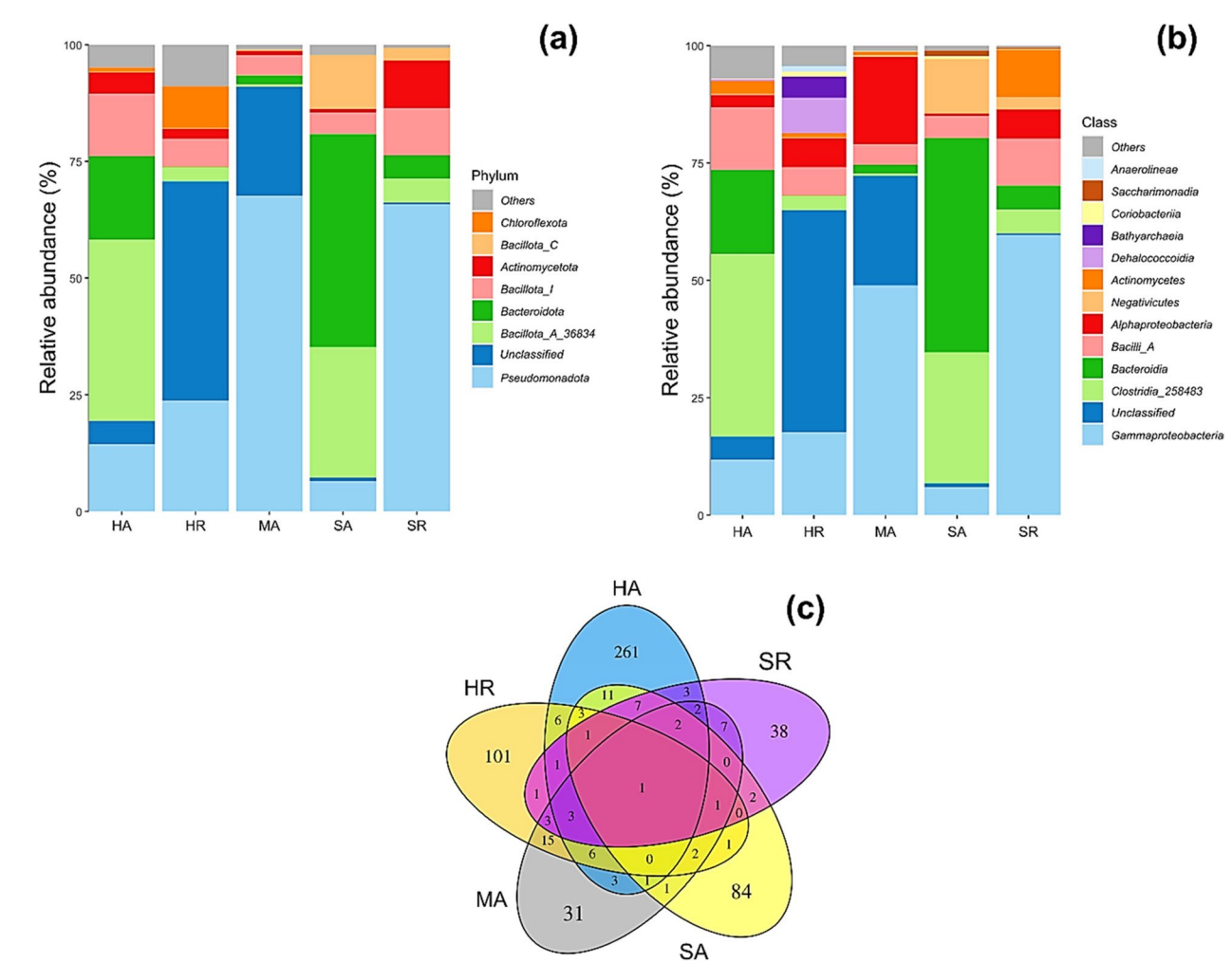


**Fig. 3** Relative abundance of dominant **a** phyla and **b** classes of bacteria identified through the 16S rRNA gene V3-V4 hypervariable region annotated through the Greengenes2 database; **c** Venn diagram of unique and shared operational taxonomic units (OTUs). Loca-

tions and mangrove species: HA (Hamata, *Avicennia marina*), HR (Hamata, *Rhizophora mucronata*), MA (Mangrove Bay, *Avicennia marina*), SA (Saffaga, *Avicennia marina*), SR (Saffaga, *Rhizophora mucronata*)

the microbial community at different locations and mangrove species is presented in Fig. 5. The RDA showed that microbial communities were different as per the relationship with the environmental variables. At the class level (Fig. 5a), *Negativicutes* were positively correlated with Cd in sediment samples collected around *A. marina* in Saffaga, whereas *Alphaproteobacteria* and *Actinomycetes* were positively correlated with Cu and Co in sediment samples collected around *A. marina* and *R. mucronata* in Mangrove Bay and Saffaga, respectively. At the genus level (Fig. 5b), *Streptococcus*, *Clostridium\_T*, and *Chryseobacterium\_A\_796612* were positively correlated with Cd in sediment samples collected around *A. marina* in Hamata. Furthermore, *Cognaticolwellia* and *Colwellia\_A\_665065* were positively correlated with Cu in sediment samples collected around *A. marina* in Mangrove Bay.

## Functional prediction

Using the FAPROTAX database, microbial species were mapped to established metabolic pathways and other ecologically significant functions, and the results are summarized in Fig. 6a. Of the five clusters, cluster 1 (Energy source) and cluster 2 (Carbon cycle) showed a higher abundance of microbial species across all samples. Cluster 1 was composed of “anaerobic chemoheterotrophy” and “aerobic chemoheterotrophy,” whereas cluster 2 comprised “xylanolysis,” “oil bioremediation,” “methylo trophy,” “methanotrophy,” “methanogenesis,” “hydrocarbon degradation,” “fermentation,” “chitinolysis,” and “cellulolysis.” The microbial composition involved in anaerobic chemoheterotrophy and fermentation was higher in SR, followed by MA, HA, HR, and SA, respectively. Figure 6b presents the predicted functional correlation with HMs. Co showed strong and positive



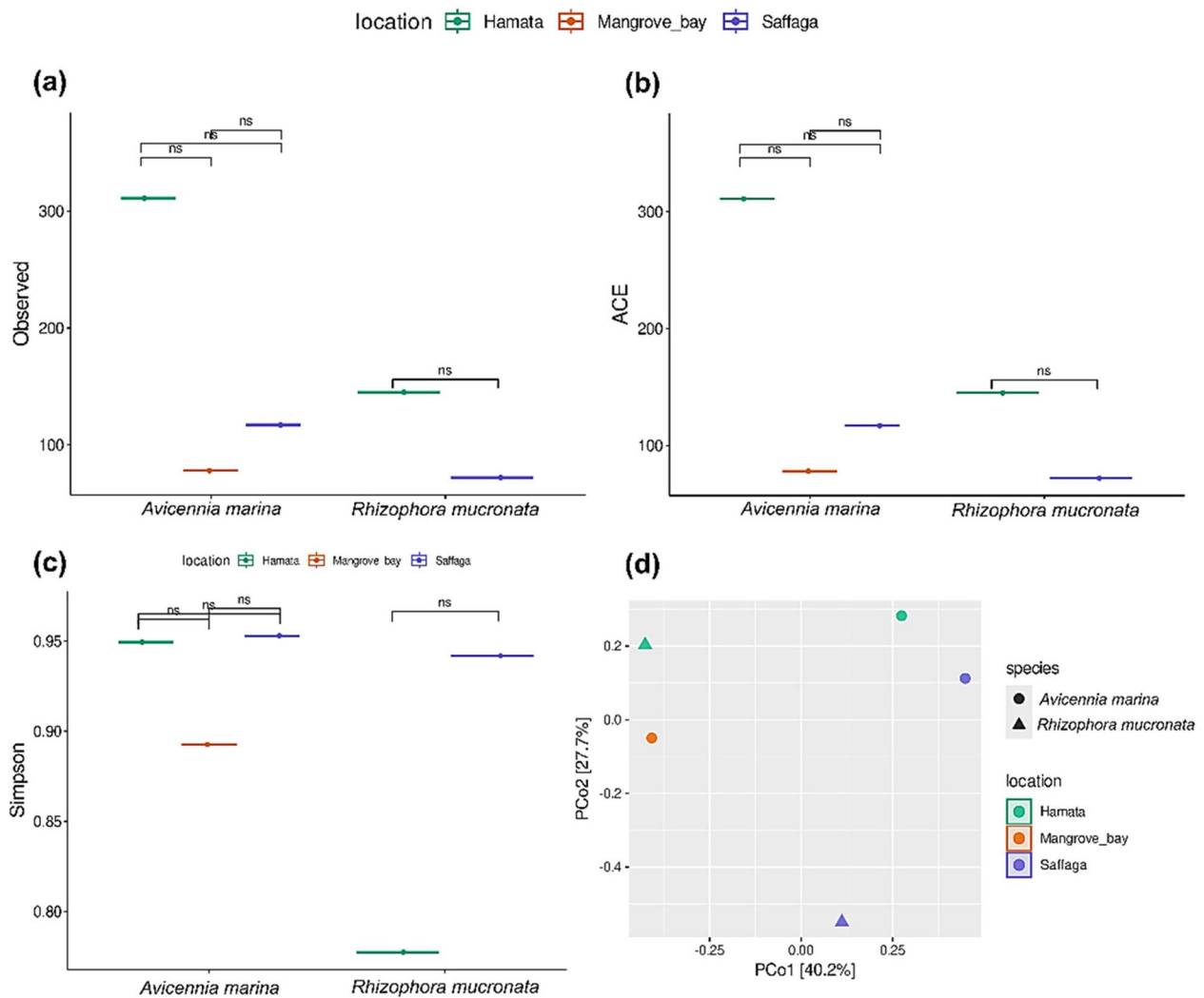


**Fig. 4** Alpha and beta diversity plots. **a** Plots corresponding to the Observed index, **b** plots corresponding to the ACE index, **c** plots corresponding to the Simpson index, and **d** principal coordinate analysis corresponding to the Bray–Curtis dissimilarity index (beta diversity).

Statistical analysis using the Kruskal–Wallis test with Benjamini–Hochberg correction for multiple comparisons (false discovery rate); ns, not significant

correlations with anaerobic chemoheterotrophy, fermentation, oil bioremediation, and ureolysis. Fe showed strong and positive correlations with xylanolysis, methanogenesis by carbon dioxide (CO<sub>2</sub>) reduction with hydrogen, hydrogenotrophic methanogenesis, and methanogenesis. Meanwhile, Mn and Zn showed a positive and strong correlation with chitinolysis.

Tax4Fun2 database was used to predict the function of unique OTUs in each sediment sample and results are presented in Fig. 7. The common functions shared by the unique OTUs in sediment samples were global and overview maps, carbohydrate metabolism, amino acid metabolism, membrane transport, energy metabolism, signal transduction, metabolism of cofactors and vitamins,

cellular community prokaryotes, lipid metabolism, nucleotide metabolism, translation, replication and repair. However, unique OTUs involved in xenobiotic biodegradation and repair and metabolism for other amino acids were abundant in most sediment samples except for SA. Unique OTUs involved in the metabolism of terpenoids and polyketides were only abundant in HA and HR sediment samples. Likewise, unique OTUs involved in the biosynthesis of other secondary metabolites were abundant in only the MA and SA sediment samples. SA sediment samples had a high abundance of unique OTUs involved in glycan biosynthesis and metabolism and cell motility. In the same regard, SR sediment samples had a high abundance of OTUs involved in folding, sorting, and degradation.

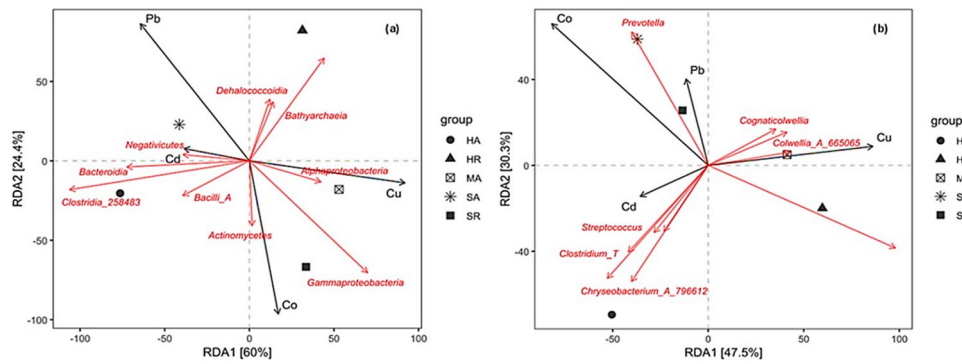


**Fig. 5** Redundancy discrimination analysis depicting the relationship between environmental variables and **a** classes and **b** genera of bacteria in different locations and mangrove species. Environmental variables that significantly explained the variability in the composition of the microbial community were fitted to the ordination. Arrows indicate the magnitude and direction of environmental variables

associated with different bacterial classes and genera. Locations and mangrove species: HA (Hamata, *Avicennia marina*), HR (Hamata, *Rhizophora mucronata*), MA (Mangrove Bay, *Avicennia marina*), SA (Saffaga, *Avicennia marina*), SR (Saffaga, *Rhizophora mucronata*). Heavy metals: Cu, copper; Pb, lead; Fe, iron; Mn, manganese; Zn, zinc; Cd, cadmium; and Co, cobalt

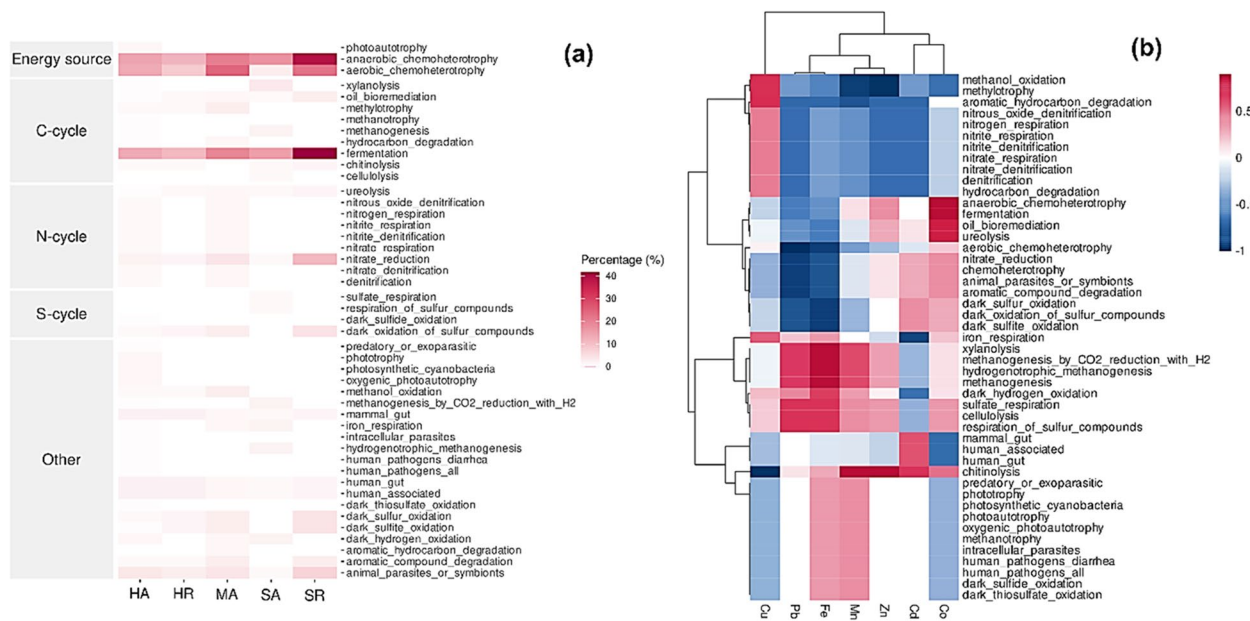


**Fig. 6** Heat-map visualization for **a** predicted functional pathways of 5 samples and **b** predicted functional correlation with heavy metals. Red colors indicate positive associations, whereas blue colors indicate negative associations. Heavy metals: Cu, copper; Pb, lead; Fe, iron; Mn, manganese; Zn, zinc; Cd, cadmium; and Co, cobalt. Loca-

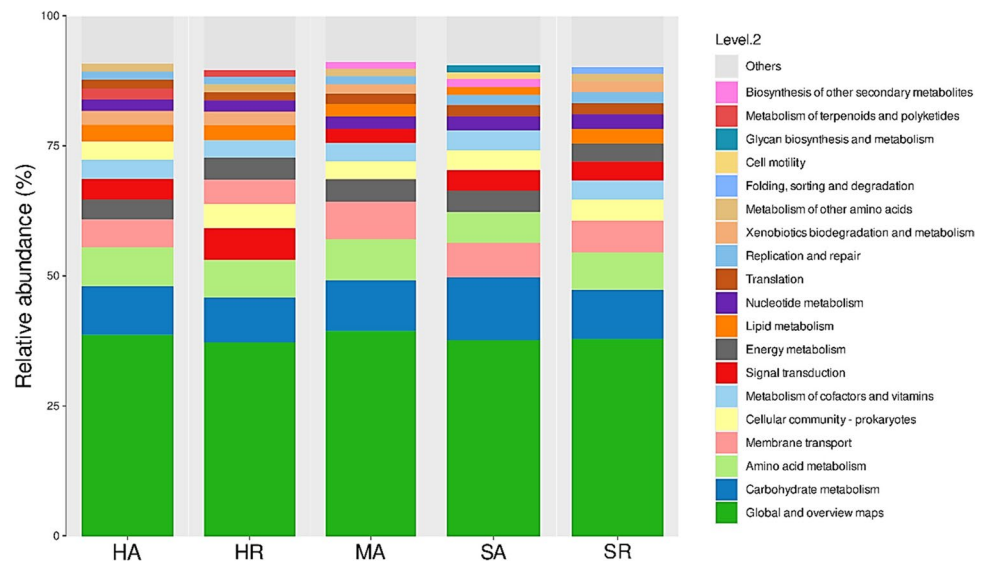
tions and mangrove species: HA (Hamata, *Avicennia marina*), HR (Hamata, *Rhizophora mucronata*), MA (Mangrove Bay, *Avicennia marina*), SA (Saffaga, *Avicennia marina*), SR (Saffaga, *Rhizophora mucronata*)

## Discussion

Microorganisms are crucial in maintaining the global biogeochemical cycling of nutrients in mangrove ecosystems (Aprilia et al. 2022; Meng et al. 2022; Yan et al. 2024). Their presence and activities are essential in the maintenance, conservation, and restoration of mangrove ecosystems (Holguin et al. 2001; Chen et al. 2016; Anu et al.

2024). In these ecosystems, bacteria and fungi are the most dominant microbes, comprising 91% of the total microbes present, followed by algae (7%) and protozoa (2%), respectively (Alongi et al. 1993; Nimnoi and Pongsilp 2022). However, microbial composition, diversity, and function in mangrove ecosystems are dependent on other environmental factors such as mangrove species, salinity, pH,

**Fig. 7** Functional prediction of unique operational taxonomic units found in sediment samples. Locations and mangrove species; HA (Hamata, *Avicennia marina*), HR (Hamata, *Rhizophora mucronata*), MA (Mangrove Bay, *Avicennia marina*), SA (Saffaga, *Avicennia marina*), SR (Saffaga, *Rhizophora mucronata*)



electroconductivity (EC), anions and cations, elements, organic carbon (OC), and bulk density (BD).

In this study, the pH of the sediment samples ranged from 8.03 to 8.33 thus indicating the slight alkalinity of mangrove sediments along the Egyptian Red Sea coast at the mangrove sites of Hamata, Mangrove Bay, and Saffaga. This is consistent with previous studies on mangrove soils along the Red Sea coast of Saudi Arabia (Zhang et al. 2009; Sohaib et al. 2023), the Egyptian-African Red Sea coast (Afele et al. 2019), and mangrove forest soil in Balandra Beach, Mexico (Gonzalez-acosta et al. 2006). However, slight acidity of mangrove soils has been reported in Ogle and Montrose (pH of 6.45 and 6.65) (Dookie et al. 2024), in a mangrove swamp (pH of 5.30 to 6.80) in Nigeria (Ukpong 2007), and a non-mangrove rehabilitation site (pH of 5.90) in Indonesia (Dewiyanti et al. 2021). The best pH value for the successful growth of mangrove trees is approximately 6 to 8.50 since this pH range is favorable for aquatic life and microbial activity (Prihastanti et al. 2021). Electroconductivity (EC) indirectly influences the availability of nutrients for plant uptake as high and low EC values hinder and support nutrient absorption by plant roots respectively (do Carmo et al. 2024). The EC reported in this study ranged from 10.42 to 22.53 dS/m which is within the range of that reported in other studies along the Red Sea coastline (Abd Ellatif et al. 2023; Sohaib et al. 2023) but below that reported by Afele et al. (2019). *A. marina* and *R. mucronata* species generally thrive in high and moderate salinity ranges of 5–35 ppt and 20–25 ppt, respectively, which translates to the EC value ranges of 8–55 dS/m for *A. marina* and 32–40 dS/m for *R. mucronata*. As such, the EC values reported in this study tend to favor *A. marina* more than they would favor *R. mucronata* and this could explain why *A. marina* has thrived better

than *R. mucronata* along the Egyptian Red Sea coastline. The bulk density (BD) of mangrove sediments ranged from 1.28 to 1.46 g/cm<sup>3</sup> across the different depths, with significant differences observed at a 30–50 cm depth. Our study results are comparable to those of Eid and Shaltout (2016) who reported BD values of mangrove stands (*Avicennia marina*) along the Egyptian Red Sea coast to range from 1.00 to 1.50 g/cm<sup>3</sup>. The dense biomass of *A. marina* and *Rhizophora mucronata* root systems reduce sediment BD because of increasing biological activities that facilitate the conservation of some micropores into macropores due to the cementing action of polysaccharides and organic acids secreted during the decomposition of organic matter (OM) by microorganisms (Sombrero and Benito 2010; Eid and Shaltout 2016). On the other hand, the sediment organic carbon (OC) percentage was higher in the upper depths (0–15 cm and 15–30 cm) than in lower depths (50–100 cm) for HA (Hamata; *A. marina*) and HR (Hamata; *R. mucronata*) sediment samples which is consistent with previous studies (Islam and Rempei 2007; Eid and Shaltout 2013; Wang et al. 2013; Lunstrum and Chen 2014; Yang et al. 2014). Most carbon inputs occur in the upper soil surface. Moreover, the upper soil surface (0–10 cm) accounts for approximately 35% of the mean total OC content which confirms its significant role in the carbon cycle (i.e., carbon sink and release of carbon dioxide) (Eid and Shaltout 2016; Saini et al. 2021; Brahim et al. 2022). However, our study results also show variations in the OC percentage in sediment samples of MA (Mangrove Bay; *A. marina*), SA (Saffaga; *A. marina*), and SR (Saffaga; *R. mucronata*) at different depths. This variation is attributed to several factors such as leaching, soil erosion, nutrient cycling, soil illuviation, mineral weathering, and decomposition (Girmay and Singh 2012).

This study also assessed the concentration of heavy metals (HMs) in sediment samples at different depths. We found that the average concentration of HMs in mangrove sediment samples ranked from the highest to the lowest were iron (Fe; 9.49 ppm) > cobalt (Co; 2.44 ppm) > lead (Pb; 1.86 ppm) > manganese (Mn; 1.37 ppm) > cadmium (Cd; 0.62 ppm) > zinc (Zn; 0.61 ppm) > copper (Cu; 0.11 ppm). This ranking corresponds to that of Nimnoi and Pongsilp (2022) and Lertprasert (2006), who found that the concentration of HMs in mangrove soils along the upper Gulf of Thailand and sediment of the Phi Lok Canal system of Samutsongkhram province, Thailand, were ranked from highest to lowest: Fe > Zn > Cu. The HMs in mangrove ecosystems are mainly from human activities such as chemical dumping, shipping, industrial waste, and urban runoff (Macfarlane and Burchett 2001; Caregnato et al. 2008). The observed concentrations of HMs in sediment samples were below the permissible limits in agricultural soils as per the standards of the World Health Organization (WHO) (Ogunlana et al. 2020). This means that the mangrove forest sites of Hamata, Mangrove Bay, and Saffaga are still free from contamination for the aforementioned HMs, and caution must be taken to avoid potential contamination. This is because the accumulation of HMs in the soil or aquatic environments through surface runoff increases the risk of their absorption by living organisms, leading to cell toxicity and neurodegenerative diseases (Rehman et al. 2021; Ohiagu et al. 2022; Jomova et al. 2025). Overall, our results on the HM concentration in mangrove sediment samples are somewhat comparable to those of El-said & Youssef (2013) and El-Sorogy et al. (2024) who carried out similar studies along the Egyptian Red Sea coast.

In this study, we also found the relation of HMs to bacterial diversity in each sediment sample collected from the studied sampling sites. Some HMs have been found to play a significant role in bacterial metabolic pathways, whereas others are toxic or non-essential (Igiri et al. 2018; Henao and Ghneim-herrera 2021; Orji et al. 2021). Moreover, bacteria have been observed to convert toxic metal ions into their respective non-toxic forms via an ATP-dependent pathway (Igiri et al. 2018; Thai et al. 2023; Fatima et al. 2024; Tang et al. 2024). *Actinomycetes* were found to be influenced by high concentrations of Co in Saffaga (Fig. 5a). This group of microbes is not only known for its production of antibiotics and other useful metabolites but also expresses plasmid-encoded genes involved in heavy metal resistance via several strategies, such as enzymatic detoxification, active transport efflux pumps, exclusion by permeability barriers, as well as intra- and extracellular sequestration (Lin et al. 2021; Gillieatt and Coleman 2024; Nnaji et al. 2024). *Negativicutes* belonging to the phylum *Bacillota* were found to be influenced by Cd, which is one of the global and most serious HM contaminants. *Bacillota* have been reported to

induce Cd resistance or participate in Cd immobilization in contaminated soils (Li et al. 2021b). The application of *Bacillota* could aid in the bioremediation of Cd-contaminated soils (Ma et al. 2023). *Prevotella*, which belongs to the phylum *Bacteroidota* were found to be influenced by Pb. *Bacteroidota* is also one of the most dominant bacterial phyla in heavy metal-contaminated environments. This is because most of the species in *Bacteroidota* can generate nutrients from their chemoheterotrophic pathways and, thus, are relatively tolerant to HM stress (Li et al. 2022a).

The metagenomics dataset of sediment samples in this study revealed that the numbers of observed species and bacterial diversity and richness in sampling sites of Hamata, Mangrove Bay, and Saffaga were not significantly different from each other, mainly due to the similarity in dominant mangrove species and mixed land use. All sites were utilized in different categories of land use, such as urbanization, agriculture, and tourism. *Pseudomonadota* (synonym "*Pseudomonadota*") was the dominant phylum, followed by *Bacteroidota* (synonym "*Bacteroidota*"), *Bacillota\_A\_368345* and *Bacillota\_I* (synonym "*Bacillota*"), *Actinomycetota* (synonym "*Actinobacteria*"), and *Chloroflexota* (synonym "*Chloroflexi*"). This result corresponds to previous studies on mangrove ecosystems. For instance, Nimnoi and Pongslip (2022) reported that the phylum *Pseudomonadota* was the most abundant, followed by *Desulfobacterota*, *Bacteroidota*, *Chloroflexi*, *Crenarchaeota*, *Acidobacteriota*, *Bacillota*, *Myxococcota*, *Gemmatimonadota*, and *Halobacterota* in mangrove forest soils along the upper Gulf of Thailand. Alghamdi et al. (2024) observed *Pseudomonadota*, *Bacillota*, *Desulfobacterota*, *Bacteroidota*, *Actinobacteriota*, *Myxococcota*, and *Gemmatimonadota* as the most dominant phyla in *A. marina* soil that was collected along the Saudi Arabian Red Sea coast. In another study, Thomson et al. (2022) investigated the influence of seasonal variation on the diversity and composition of bacteria in *A. marina* soils and reported *Pseudomonadota*, *Chloroflexi*, and *Bacteroidota* as the most dominant phyla in the surface and subsurface soils in both summer and winter seasons. In *Rhizophora mucronata* soils, Allaouia et al. (2022) found *Pseudomonadota*, *Desulfobacteria*, *Bacteroidota*, and *Chloroflexota* as some of the most abundant phyla. In the Indian mangrove system, Ghosh et al. (2022) reported *Pseudomonadota*, *Bacillota*, *Bacteroidota*, and *Actinobacteria* as the most abundant phyla. Overall, these results indicate that *Pseudomonadota* is the most predominant and cosmopolitan bacterial phylum in diverse mangrove environments. *Pseudomonadota* are metabolically diverse and can survive in different ecosystems due to the presence of different groups of genes in their DNA responsible for stress resistance (Ghosh et al. 2022). On the other hand, we also observed a significant relative abundance of unclassified bacteria at the phylum and class levels in HR and MA sediment samples. Unclassified



bacteria are common in environmental microbiome analysis (Pu et al. 2024). Delgado-Baquerizo (2019) conducted a global soil survey of 235 sites and concluded that 99% of bacterial phylotypes could not be taxonomically classified, especially in boreal and tropical forests. The authors attributed this to environmental factors such as precipitation, temperature, pH, and soil nutrient content and texture that could lead to an increased abundance of these unclassified microbes. Soil nutrient and texture analysis revealed high concentrations of nitrogen in HR and MA sediment samples (Supplementary Table 1), which could have led to this observation. High nitrogen levels influence microbial composition in sediments, potentially leading to a higher abundance of unclassified bacteria. This is because excess nitrogen alters the sediment's chemical properties, which in turn favors the proliferation of certain bacterial groups while potentially hindering others. These shifts in microbial community structure can be observed through changes in the relative abundance of different bacterial phyla (Wang et al. 2018; Lin et al. 2019).

Our analysis revealed significant variations in microbial community composition across the study sites (Fig. 3a, b). For instance, the high abundance of *Pseudomonadota* (67.6%) at Mangrove Bay (MA) and *Bacteroidota* (45.9%) at Saffaga (SA) suggests that local site conditions are shaping distinct communities. These differences correlate with variations in environmental factors. The redundancy analysis (RDA) (Fig. 5) showed that the high levels of copper at Mangrove Bay strongly influenced its microbial structure, which was dominated by copper-tolerant genera like *Cognatibacillus* and *Colwellia\_A* (Supplementary Table 2). Similarly, the Saffaga sites (SA, SR) showed elevated cobalt levels, which correlated with a higher abundance of *Actinomyces* (Fig. 5a), a phylum known to include metal-resistant members. These shifts in community structure are directly reflected in the metabolic potential for each community. The high abundance of *Pseudomonadota* and *Bacteroidota* across all sites, which are known to be metabolically versatile, explains the dominance of broad metabolic functions like “aerobic chemoheterotrophy” and “fermentation” observed in the FAPROTAX analysis (Fig. 6a).

Gammaproteobacteria and Alphaproteobacteria were the most dominant classes in SR and MA sediment samples, respectively (Fig. 3b), and these have been reported to play a vital role in biogeochemical cycles, especially in the nitrogen and carbon cycle (Dyksma et al. 2016; Goethem et al. 2017). The class *Bacteroidia*, which was more dominant in SA, has been previously reported for its attributes, such as wide distribution in different environments (sediments, soil, and seawater), the ability to biosynthesize acetic and succinic acid and proteolytic activity (Mendes et al. 2013; Nimnoi and Pongsilp 2022). Microbial biosynthesis of succinic acid via the reverse TCA (Tricarboxylic acid cycle)

promotes carbon dioxide fixation, thus an important process in carbon sequestration (Malubhoy et al. 2022). *Clostridia*, which are the dominant class in HA, include bacterial genera that have been previously reported to play a role in the sulfur cycle (Sallam and Steinbu 2009). The predicted functional correlation with HMs showed high positive correlations of Co to fermentation and oil bioremediation (Fig. 6b). Co has been previously reported to enhance rumen microbial fermentation of substrates in animals (Ryazanov et al. 2022; Wang et al. 2022b; Zhang et al. 2023). Likewise, Co plays a role in the metabolism of methanogenic bacteria (Paulo et al. 2017), which includes species that have been reported to degrade oils in contaminated environments (Sherry et al. 2020; Suda et al. 2021). Fe is another HM which showed a strong positive correlation to methanogenesis. Depending on its form, Fe can promote or hinder methanogenesis in natural anaerobic environments (Baek et al. 2019). Mn and Zn were also found to have a strong and positive correlation to chitinolysis. Chitinolytic bacteria play a significant role in the biodegradation of chitin, one of the most predominant polymers in nature. These microbes synthesize specific enzymes that catalyze the hydrolysis of beta-1,4-glycosidic bonds in low-digestible chitin polymers (Brzezinska et al. 2014; Dhole et al. 2021). The presence of Mn in specific concentrations could enhance the enzyme production of chitinolytic bacteria. Kuddus and Ahmad (2013) observed that the addition of  $Mn^{2+}$  in the culture media enhanced chitinase production. However, unlike the results of this study, Zn has been previously reported to inhibit chitinase production (Poria et al. 2021; Ekundayo et al. 2022).

## Limitations of this study

- Sediment samples were collected in only one season. Assessment of changes in microbial diversity and predicted function over multiple seasons would provide new insights into the impact of various environmental factors on the sediment microbial profile.
- Sampling from undisturbed mangrove forests along the Egyptian Red Sea coastline and comparing their sediment microbial profile with the data of this study would lead to the identification of shared and different microbial taxa present in these locations.
- 16S rRNA gene sequencing was used for microbial phylogeny and functional prediction. This approach does not capture the entire DNA of the microbes, allowing for a broader view of the microbes present, their functional genes, and metabolic pathways.
- Whereas Greengenes2 presents a significant advancement in unifying microbial data through a single reference tree, it still presents certain limitations in the taxo-



onomic coverage for less well-characterized environments or organisms not extensively represented in the underlying databases, as well as the inability to classify organisms to a species level.

## Conclusion

This study sheds light on the physiochemical properties, microbial and functional diversity of mangrove sediments along the Egyptian Red Sea coastal areas of Hamata, Mangrove Bay, and Saffaga. Our findings revealed a similarity in the concentration of the measured physiochemical properties among the sediment samples across all depths except for the 30–50 cm depth. Heavy metal analysis showed higher and lower concentrations of copper and iron, lead, manganese, and zinc, respectively, in sediment samples collected in Mangrove Bay compared to those collected in Hamata and Saffaga, thus indicating the role of human activities (i.e., tourism and urbanization) in heavy metal contamination of mangrove ecosystems. All the sediment samples shared similarities in the predominant microbial taxa. Still, they differed in their relative abundance, thus indicating the influence of mangrove species, proximity to the shoreline, and human activity on microbial composition. Furthermore, heavy metals have a significant influence on microbial activity in the mangrove ecosystem; hence, care should be taken in the conservation and restoration of mangrove ecosystems. Further studies are needed to decipher changes in the microbial composition, diversity, and function in different seasons.

**Supplementary information** The online version contains supplementary material available at <https://doi.org/10.1007/s11356-025-37234-1>.

**Acknowledgements** The authors wish to thank Abdallah El-qut, Mostafa Metwally, and Walaa Ahmed for their assistance in the sediment sample collection and DNA extractions during this project.

**Author contribution** Conceptualization: Muziri Mugwanya and Eric Zadok Mpingirika; formal analysis and investigation: Muziri Mugwanya, Eric Zadok Mpingirika, Rafat A. Eissa, and Yasmine AbdelMaksoud; writing—original draft preparation: Muziri Mugwanya; writing—review and editing: Muziri Mugwanya, Eric Zadok Mpingirika, Rafat A. Eissa, and Yasmine AbdelMaksoud; funding acquisition: Hani Sewilam; resources: Hani Sewilam; supervision: Yasmine AbdelMaksoud and Hani Sewilam.

**Funding** Open Access funding enabled and organized by Projekt DEAL. The work was funded through the project “Developing Participatory Mangrove Ecosystem Restoration Model as a Nature-Based Solution to Climate Change (MERS).”

**Data availability** Microbiological datasets associated with this work have been deposited at the Sequence Read Archive (SRA) of the National Center for Biotechnology Information (NCBI) and are publicly available under the BioProject ID PRJNA1224588. Data sets on

the physiochemical properties and heavy metals are publicly available at <https://data.mendeley.com/datasets/95zjycf9gh/1>.

## Declarations

**Ethical approval** N/A.

**Consent to participate** N/A.

**Consent for publication** N/A.

**Competing interests** The authors declare no competing interests.

**Open Access** This article is licensed under a Creative Commons Attribution 4.0 International License, which permits use, sharing, adaptation, distribution and reproduction in any medium or format, as long as you give appropriate credit to the original author(s) and the source, provide a link to the Creative Commons licence, and indicate if changes were made. The images or other third party material in this article are included in the article's Creative Commons licence, unless indicated otherwise in a credit line to the material. If material is not included in the article's Creative Commons licence and your intended use is not permitted by statutory regulation or exceeds the permitted use, you will need to obtain permission directly from the copyright holder. To view a copy of this licence, visit <http://creativecommons.org/licenses/by/4.0/>.

## References

- Abd Ellatif AA, Mousa KF, Merwad AM, Saeed Abohashim (2023) Mangrove ecosystem effect on soil physico-chemical properties at the Red Sea coast. *Int J Chem Biochem Sci* 24:555–564. <https://www.iscientific.org/wp-content/uploads/2024/04/56-ijcbs-23-24-12-56n.pdf>. Accessed 5 Nov 2024
- Afele AA, Abbas MS, Soliman AS, Khedr AH, Hatab EB (2019) Physical and chemical characteristics of mangrove soil under marine influence. A case study on the mangrove forests at Egyptian-African Red Sea coast. *Egypt J Aquat Biol Fish* 23:385–399
- Ahmed S, Kamruzzaman M, Rahman MS, Sakib N, Azad MS, Dey T (2022) Nature-based solutions stand structure and carbon storage of a young mangrove plantation forest in coastal area of Bangladesh : the promise of a natural solution. *Nature-Based Solut* 2:100025. <https://doi.org/10.1016/j.nbsj.2022.100025>
- Alam K, Abbasi MN, Hao J, Zhang Y, Li A (2021) Strategies for natural products discovery from uncultured microorganisms. *Molecules* 26:2977. <https://doi.org/10.3390/molecules26102977>
- Alghamdi AK, Parween S, Hirt H, Saad MM (2024) Unveiling the bacterial diversity and potential of the *Avicennia marina* ecosystem for enhancing plant resilience to saline conditions. *Environ Microbiol* 19(1):101. <https://doi.org/10.1186/s40793-024-00642-w>
- Allaouia ASA, Raissa S, Fahimat SH, Asnat S, Mohamed A, Abdou NM, Ismail SS, Karima YA, Aladine BH, Mohamed NA, Elyamine AM (2022) *Int J Adv Eng Res Sci* 9:79–89. <https://doi.org/10.22161/ijaers.98.11>
- Alongi DM, Christoffersen P, Tirendi F (1993) The influence of forest type on microbial-nutrient relationships in tropical mangrove sediments. *J Exp Mar Biol Ecol* 171:201–223. [https://doi.org/10.1016/0022-0981\(93\)90004-8](https://doi.org/10.1016/0022-0981(93)90004-8)
- Anu K, Sneha VK, Busheera P (2024) Mangroves in environmental engineering: harnessing the multifunctional potential of nature's coastal architects for sustainable ecosystem management. *Results Eng* 21:101765. <https://doi.org/10.1016/j.rineng.2024.101765>

- Aprilia D, Arifiani KN, Dianti D, Cahyaningsih AP, Kusumaningrum L, Sarno S, Rahim KA, Setyawan AD (2022) Biogeochemical process in mangrove ecosystem. *Int J Bonorowo Wetl* 10:126–141. <https://doi.org/10.13057/bonorowo/w100205>
- Baek G, Kim J, Lee C (2019) A review of the effects of iron compounds on methanogenesis in anaerobic environments. *Renew Sustain Energy Rev* 113:109282. <https://doi.org/10.1016/j.rser.2019.109282>
- Baskaran V, Mahalakshmi A, Prabavathy VR (2023) Rhizosphere mangroves: a hotspot for novel bacterial and archaeal diversity. *Rhizosphere* 27:100748. <https://doi.org/10.1016/j.rhisph.2023.100748>
- Bolyen E, Rideout JR, Dillon MR, Bokulich NA, Abnet CC, Al-Ghalith GA, Alexander H, Alm EJ, Arumugam M, Asnicar F, Bai Y (2019) Reproducible, interactive, scalable and extensible microbiome data science using QIIME 2. *Nat Biotechnol* 37:1091. <https://doi.org/10.1038/s41587-019-0252-6>
- Brahim N, Ibrahim H, Mlih R, Bouajila A, Karbout N, Bol R (2022) Soil OC and N stocks in the saline soil of Tunisian Gataaya Oasis eight years after application of manure and compost. *Land* 11:442. <https://doi.org/10.3390/land11030442>
- Brzezinska MS, Jankiewicz U, Burkowska A, Walczak M (2014) Chitinolytic microorganisms and their possible application in environmental protection. *Curr Microbiol* 68:71–81. <https://doi.org/10.1007/s00284-013-0440-4>
- Caregnato FF, Koller CE, Macfarlane GR, Moreira JCF (2008) The glutathione antioxidant system as a biomarker suite for the assessment of heavy metal exposure and effect in the grey mangrove, *Avicennia marina* (Forsk.) Vierh. *Mar Pollut Bull* 56:1119–1127. <https://doi.org/10.1016/j.marpolbul.2008.03.019>
- Chatting M, Al-Maslmani I, Walton M, Skov MW, Kennedy H, Husrevoglu YS, Le Vay L (2022) Future mangrove carbon storage under climate change and deforestation. *Front Mar Sci* 9:1–14. <https://doi.org/10.3389/fmars.2022.781876>
- Chen Q, Zhao Q, Li J, Jian S, Ren H (2016) Mangrove succession enriches the sediment microbial community in South China. *Sci Rep* 6:1–9. <https://doi.org/10.1038/srep27468>
- Dajam AS, Keshta AE, Bindajam AA, Eid EM (2024) Bioaccumulation of heavy metals in mangrove (*Avicennia marina*): predictive uptake modeling and phytoremediation potential. *J Soil Sci Plant Nutr* 24:6085–6098. <https://doi.org/10.1007/s42729-024-01962-z>
- Delgado-Baquerizo M (2019) Obscure soil microbes and where to find them. *ISME J* 13:2120–2124. <https://doi.org/10.1038/s41396-019-0405-0>
- Dewiyanti, I., Darmawi, D., Muchlisin, Z. A., Helmi, T. Z., Imelda, I., & Defira, C. N. (2021, February). Physical and chemical characteristics of soil in mangrove ecosystem based on differences habitat in Banda Aceh and Aceh Besar. In *IOP Conference Series: Earth and Environmental Science* (Vol. 674, No. 1, p. 012092). IOP Publishing <https://iopscience.iop.org/article/10.1088/1755-1315/674/1/012092>
- Dhole NP, Dar MA, Pandit RS (2021) Recent advances in the bioprospection and applications of chitinolytic bacteria for valorization of waste chitin. *Arch Microbiol* 203:1953–1969. <https://doi.org/10.1007/s00203-021-02234-5>
- do Carmo AP, Freitas MS, Machado LC, dos Santos Silva L, Petri DJ, Vimercati JC, Matos CR, Mathias L, Vieira II, de Carvalho AJ (2024) Electrical conductivity of nutrient solutions affects the growth, nutrient levels, and content and composition of essential oils of *Acmella oleracea* (L.) R. K. Jansen from southeastern Brazil. *J Agric Food Res* 15:100968. <https://doi.org/10.1016/j.jafr.2024.100968>
- Dookie S, Jaikishun S, Ansari AA (2024) Soil and water relations in mangrove ecosystems in Guyana. *Geol Ecol Landscapes* 8:445–469. <https://doi.org/10.1080/24749508.2022.2142186>
- Doran JW, Mielke LN (1984) A rapid, low-cost method for determination of soil bulk density†. *Soil Sci Soc Am J* 48:717–719. <https://doi.org/10.2136/sssaj1984.03615995004800040004x>
- Dyksma S, Bischof K, Fuchs BM, Hoffmann K, Meier D, Meyerdierks A, Pjevac P, Probandt D, Richter M, Stepanauskas R, Mußmann M (2016) Ubiquitous Gammaproteobacteria dominate dark carbon fixation in coastal sediments. *ISME J* 10(8):1939–1953. <https://doi.org/10.1038/ismej.2015.257>
- Eid EM, Shaltout KH (2013) Evaluation of carbon sequestration potentiality of Lake Burullus, Egypt to mitigate climate change. *Egypt J Aquat Res* 39:31–38. <https://doi.org/10.1016/j.ejar.2013.04.002>
- Eid EM, Shaltout KH (2016) Distribution of soil organic carbon in the mangrove *Avicennia marina* (Forsk.) Vierh. along the Egyptian Red Sea Coast. *Reg Stud Mar Sci* 3:76–82. <https://doi.org/10.1016/j.rsma.2015.05.006>
- Ekundayo FO, Folorunsho AE, Ibanmi TA (2022) Antifungal activity of chitinase produced by *Streptomyces* species isolated from grassland soils in Futa Area, Akure. *Bull Natl Res Cent.* <https://doi.org/10.1186/s42269-022-00782-4>
- El-said GF, Youssef DH (2013) Ecotoxicological impact assessment of some heavy metals and their distribution in some fractions of mangrove sediments from Red Sea, Egypt. *Environ Monit Assess* 185(1):393–404. <https://doi.org/10.1007/s10661-012-2561-9>
- El-Sorogy AS, Al-Hashim MH, Almadani SA, Giacobbe S, Nour HE (2024) Potential contamination and health risk assessment of heavy metals in Hurghada coastal sediments, Northwestern Red Sea. *Mar Pollut Bull* 198:115924. <https://doi.org/10.1016/j.marpolbul.2023.115924>
- Farshid Z, Moradi Balef R, Zendejboudi T, Dehghan N, Mohajer F, Kalbi S, Hashemi A, Afshar A, Heidari Bafghi T, Baneshi H, Tamadon A (2023) Reforestation of grey mangroves (*Avicennia marina*) along the northern coasts of the Persian Gulf. *Wetl Ecol Manag* 31:115–128. <https://doi.org/10.1007/s11273-022-09904-1>
- Fatima Z, Azam A, Iqbal MZ, Badar R, Muhammad G (2024) A comprehensive review on effective removal of toxic heavy metals from water using genetically modified microorganisms. *Desalin Water Treat* 319:100553. <https://doi.org/10.1016/j.dwt.2024.100553>
- Ghose M, Parab AS, Manohar CS, Mohanan D, Toraskar A (2024) Unraveling the role of bacterial communities in mangrove habitats under the urban influence, using a next-generation sequencing approach. *J Sea Res* 198:102469. <https://doi.org/10.1016/j.seares.2024.102469>
- Ghosh A, Saha R, Bhadury P (2022) Metagenomic insights into surface water microbial communities of a South Asian mangrove ecosystem. *PeerJ* 10:e13169. <https://doi.org/10.7717/peerj.13169>
- Gillieatt BF, Coleman NV (2024) Unravelling the mechanisms of antibiotic and heavy metal resistance co-selection in environmental bacteria. *FEMS Microbiol Rev* 48:fuae017. <https://doi.org/10.1093/femsre/fuae017>
- Girmay G, Singh BR (2012) Changes in soil organic carbon stocks and soil quality: land-use system effects in northern Ethiopia. *Acta Agric Scand Sect B Soil Plant Sci* 62:519–530. <https://doi.org/10.1080/09064710.2012.663786>
- Gonzalez-acosta B, Bashan Y, Hernandez-saavedra NY, Ascencio F (2006) Seasonal seawater temperature as the major determinant for populations of culturable bacteria in the sediments of an intact mangrove in an arid region. *FEMS Microbiol Ecol* 55(2):311–321. <https://doi.org/10.1111/j.1574-6941.2005.00019.x>
- Guo C, Loh PS, Hu J, Chen Z, Pradit S, Oeuring C, Sok T, Mohamed CA, Lee CW, Bong CW, Lu X (2024) Factors influencing mangrove carbon storage and its response to environmental stress. *Front Mar Sci* 11:1410183. <https://doi.org/10.3389/fmars.2024.1410183>
- Henao SG, Ghneim-herrera T (2021) Heavy metals in soils and the remediation potential of bacteria associated with the plant

- microbiome. *Front Environ Sci* 9:604216. <https://doi.org/10.3389/fenvs.2021.604216>
- Holguin G, Vazquez P, Bashan Y (2001) The role of sediment microorganisms in the productivity, conservation, and rehabilitation of mangrove ecosystems: an overview. *Biol Fertil Soils* 33:265–278. <https://doi.org/10.1007/s003740000319>
- Hossain MB, Masum Z, Rahman MS, Yu J, Noman MA, Jolly YN, Begum BA, Paray BA, Arai T (2022) Heavy metal accumulation and phytoremediation potentiality of some selected mangrove species from the world's largest mangrove forest. *Biology* 11(8):1144. <https://doi.org/10.3390/biology11081144>
- Hu B, Liao J, Zhang Q, Ding S, He M, Qiao Y, Zhang Z, Shang C, Chen S (2022) Diversity and vertical distribution of sedimentary bacterial communities and its association with metal bioavailability in three distinct mangrove reserves of South China. *Water* 14:971. <https://doi.org/10.3390/w14060971>
- Igiri BE, Okoduwa SI, Idoko GO, Akabuogu EP, Adeyi AO, Ejiogu IK (2018) Toxicity and bioremediation of heavy metals contaminated ecosystem from tannery wastewater: a review. *J Toxic* 2018:1–16. <https://doi.org/10.1155/2018/2568038>
- Islam N, Rempei KÆ (2007) Carbon and nitrogen pools in a mangrove stand of *Kandelia obovata* (S., L.) Yong: vertical distribution in the soil – vegetation system. *Wetl Ecol Manag* 15:141–153. <https://doi.org/10.1007/s11273-006-9020-8>
- Jomova K, Alomar SY, Nepovimova E, Kuca K, Valko M (2025) Heavy metals: toxicity and human health effects. *Arch Toxicol* 99:153–209. <https://doi.org/10.1007/s00204-024-03903-2>
- Kannan P, Verma I, Banerjee B, Saleena LM (2024) Unveiling bacterial consortium for xenobiotic biodegradation from Pichavaram mangrove forest soil: a metagenomic approach. *Arch Microbiol* 206:1–11. <https://doi.org/10.1007/s00203-023-03765-9>
- Karmakar S, Riya KK, Jolly YN, Akter S, Mamun KM, Kabir J, Paray BA, Arai T, Yu J, Ngah N, Hossain MB (2025) Effectiveness of artificially planted mangroves on remediation of metals released from ship-breaking activities. *Mar Pollut Bull* 212:117587. <https://doi.org/10.1016/j.marpolbul.2025.117587>
- Kida M, Fujitake N (2020) Organic carbon stabilization mechanisms in mangrove soils: a review. *Forests* 11:981. <https://doi.org/10.3390/f11090981>
- Kuddus M, Ahmad IZ (2013) Isolation of novel chitinolytic bacteria and production optimization of extracellular chitinase. *J Genet Eng Biotechnol* 11:39–46. <https://doi.org/10.1016/j.jgeb.2013.03.001>
- Lai J, Cheah W, Palaniveloo K, Suwa R, Sharma S (2022) A systematic review of the physicochemical and microbial diversity of well-preserved, restored, and disturbed mangrove forests: what is known and what is the way forward? *Forests* 13:2160. <https://doi.org/10.3390/f13122169>
- Lertprasert N (2006) Accumulation and Distribution of Heavy Metals in Water, Sediment, *Ipomoea Aquatica* Forsk., and *Rhizophora Apiculata* Blume, in the Phi Lok Canal System, Samut Songkhram Province. Master's thesis, Faculty of Graduate Studies, Mahidol university.
- Li H, Shen Y, He Y, Gao T, Li G, Zuo M, Ji J, Li C, Li X, Chen Y, Yin Z (2022) Effects of heavy metals on bacterial community structures in two lead–zinc tailings situated in northwestern China. *Arch Microbiol* 204:1–14. <https://doi.org/10.1007/s00203-021-02699-4>
- Li L, Peng C, Yang Z, He Y, Liang M, Cao H, Qiu Q, Song J, Su Y, Gong B (2022) Microbial communities in swamps of four mangrove reserves driven by interactions between physicochemical properties and microbe in the North Beibu Gulf, China. *Environ Sci Pollut Res* 29:37582–37597. <https://doi.org/10.1007/s11356-021-18134-6>
- Li M, Fang A, Yu X, Zhang K, He Z, Wang C, Peng Y, Xiao F, Yang T, Zhang W, Zheng X (2021) Microbially-driven sulfur cycling microbial communities in different mangrove sediments. *Chemosphere* 273:128597. <https://doi.org/10.1016/j.chemosphere.2020.128597>
- Li X, Li X, Li Y, Dai X, Zhang Q, Zhang M, Zhang Z, Tao Y, Chen W, Zhang M, Zhou X (2021) Improved immobilization of soil cadmium by regulating soil characteristics and microbial community through reductive soil disinfection. *Sci Total Environ* 778:146222. <https://doi.org/10.1016/j.scitotenv.2021.146222>
- Lin Y, Wang L, Xu K, Li K, Ren H (2021) Revealing taxon-specific heavy metal-resistance mechanisms in denitrifying phosphorus removal sludge using genome-centric metaproteomics. *Microbiome* 9:1–17. <https://doi.org/10.1186/s40168-021-01016-x>
- Lin X, Gao D, Lu K, Li X (2019) Bacterial community shifts driven by nitrogen pollution in river sediments of a highly urbanized city. *Int J Environ Res Public Health* 16:3794. <https://doi.org/10.3390/ijerph16203794>
- Louca S, Jacques SM, Pires AP, Leal JS, Srivastava DS, Parfrey LW, Farjalla VF, Doebeli M (2016) High taxonomic variability despite stable functional structure across microbial communities. *Nat Ecol Evol* 1:1–12. <https://doi.org/10.1038/s41559-016-0015>
- Lunstrum A, Chen L (2014) Soil carbon stocks and accumulation in young mangrove forests. *Soil Biol Biochem* 75:223–232. <https://doi.org/10.1016/j.soilbio.2014.04.008>
- Ma B, Song W, Zhang X, Chen M, Li J, Yang X, Zhang L (2023) Potential application of novel cadmium-tolerant bacteria in bioremediation of Cd-contaminated soil. *Ecotoxicol Environ Saf* 255:114766. <https://doi.org/10.1016/j.ecoenv.2023.114766>
- Macfarlane GR, Burchett MD (2001) Photosynthetic pigments and peroxidase activity as indicators of heavy metal stress in the grey. *Mar Pollut Bull* 42:233–240. [https://doi.org/10.1016/S0025-326X\(00\)00147-8](https://doi.org/10.1016/S0025-326X(00)00147-8)
- Madeira M, Auxtero E, Sousa E (2003) Cation and anion exchange properties of Andisols from the Azores, Portugal, as determined by the compulsive exchange and the ammonium acetate methods. *Geoderma* 117:225–241. [https://doi.org/10.1016/S0016-7061\(03\)00125-3](https://doi.org/10.1016/S0016-7061(03)00125-3)
- Malubhoy Z, Bahia FM, de Valk SC, de Hulster E, Rendulić T, Ortiz JP, Xiberras J, Klein M, Mans R, Nevoigt E (2022) Carbon dioxide fixation via production of succinic acid from glycerol in engineered *Saccharomyces cerevisiae*. *Microb Cell Fact*. <https://doi.org/10.1186/s12934-022-01817-1>
- McDonald D, Jiang Y, Balaban M, Cantrell K, Zhu Q, Gonzalez A, Morton JT, Nicolaou G, Parks DH, Karst SM, Albertsen M (2024) Greengenes2 unifies microbial data in a single reference tree. *Nat Biotechnol* 42:715–718. <https://doi.org/10.1038/s41587-023-01845-1>
- Mendes R, Garbeva P, Raaijmakers JM (2013) The rhizosphere microbiome: significance of plant beneficial, plant pathogenic, and human pathogenic microorganisms. *FEMS Microbiol Rev* 37:634–663. <https://doi.org/10.1111/1574-6976.12028>
- Meng S, Peng T, Liu X, Wang H, Huang T, Gu JD, Hu Z (2022) Ecological role of bacteria involved in the biogeochemical cycles of mangroves based on functional genes detected through GeoChip 5.0. *mSphere* 7:1–12. <https://doi.org/10.1128/msphere.00936-21>
- Nafea AM, Wang Y, Wang D, Salama AM, Aziz MA, Xu S, Tong Y (2024) Application of next-generation sequencing to identify



- different pathogens. *Front Microbiol* 14:1329330. <https://doi.org/10.3389/fmicb.2023.1329330>
- Nimnoi P, Pongsilp N (2022) Insights into bacterial communities and diversity of mangrove forest soils along the upper Gulf of Thailand in response to environmental factors. *Biology (Basel)* 11:1–22. <https://doi.org/10.3390/biology11121787>
- Nnaji ND, Anyanwu CU, Miri T (2024) Mechanisms of heavy metal tolerance in bacteria: a review. *Sustainability* 16:11124. <https://doi.org/10.3390/su162411124>
- Ogunlana R, Korode AI, Ajibade ZF (2020) Assessing the level of heavy metals concentration in soil around transformer at Akoko Community of Ondo State, Nigeria. *J Appl Sci Environ Manag* 24:2183–2189. <https://doi.org/10.4314/jasem.v24i12.26>
- Ohiagu FO, Chikezie PC, Ahaneku CC, Chikezie CM (2022) Human exposure to heavy metals: toxicity mechanisms and health implications. *Mater Sci Eng Int J* 6:78–87. <https://doi.org/10.15406/msej.2022.06.00183>
- Orji OU, Awoke JN, Aja PM, Aloke C, Obasi OD, Alum EU, Udu-Ibiam OE, Oka GO (2021) Halotolerant and metalotolerant bacteria strains with heavy metals bioremediation possibilities isolated from Uburu Salt Lake, Southeastern, Nigeria. *Heliyon* 7(7):e07512. <https://doi.org/10.1016/j.heliyon.2021.e07512>
- Padhy SR, Bhattacharyya P, Dash PK, Nayak SK, Parida SP, Baig MJ, Mohapatra T (2022) Elucidation of dominant energy metabolic pathways of methane, sulphur and nitrogen in respect to mangrove-degradation for climate change mitigation. *J Environ Manage* 303:114151. <https://doi.org/10.1016/j.jenvman.2021.114151>
- Park C, Kim SB, Choi SH, Kim S (2021) Comparison of 16S rRNA gene based microbial profiling using five next-generation sequencers and various primers. *Front Microbiol* 12:715500. <https://doi.org/10.3389/fmicb.2021.715500>
- Patil V, Singh A, Naik N, Seema U, Sawant B (2012) Carbon sequestration in mangroves ecosystems. *J Environ Res Dev* 7:576–583
- Paulo LM, Ramiro-Garcia J, van Mourik S, Stams AJ, Sousa DZ (2017) Effect of nickel and cobalt on methanogenic enrichment cultures and role of biogenic sulfide in metal toxicity attenuation. *Front Microbiol* 8:1341. <https://doi.org/10.3389/fmicb.2017.01341>
- Poria V, Rana A, Kumari A, Grewal J, Pranaw K, Singh S (2021) Current perspectives on chitinolytic enzymes and their agro-industrial applications. *Biology (Basel)* 10:1319. <https://doi.org/10.3390/biology10121319>
- Prihastanti E, Hastuti ED, Haryanti S, Purnomo, SP (2021, July) The anatomic response of the mangrove vegetation due to the changing in land functions. In *Journal of Physics: Conference Series* (Vol. 1943, No. 1, p. 012061). IOP Publishing. <https://iopscience.iop.org/article/10.1088/1742-6596/1943/1/012061/meta>
- Pu W, Wang M, Song D, Zhao W, Sheng X, Huo T, Du X, Sui X (2024) Bacterial diversity in sediments from Lianhuan Lake, Northeast China. *Microorganisms* 12:1–19. <https://doi.org/10.3390/microorganisms12091914>
- Raju K, Sekar J, Ramalingam PV (2016) *Salinicola rhizosphaerae* sp. nov., isolated from the rhizosphere of the mangrove *Avicennia marina* L. *Int J Syst Evol Microbiol* 66:1074–1079. <https://doi.org/10.1099/ijsem.0.000837>
- Rehman AU, Nazir S, Irshad R, Tahir K, ur Rehman K, Islam RU, Wahab Z (2021) Toxicity of heavy metals in plants and animals and their uptake by magnetic iron oxide nanoparticles. *J Mol Liq* 321:114455. <https://doi.org/10.1016/j.molliq.2020.114455>
- Rognes T, Flouri T, Nichols B, Quince C, Mahé F (2016) VSEARCH: a versatile open source tool for metagenomics. *PeerJ* 2016:1–22. <https://doi.org/10.7717/peerj.2584>
- Ryazanov V, Duskaev G, Sheida E, Nurzhanov B, Kurilkina M (2022) Rumen fermentation, methane concentration, and blood metabolites of cattle receiving dietetical phytobiotic and cobalt (II) chloride. *Vet World* 15:2551–2557. <https://doi.org/10.14202/vetworld.2022.2551-2557>
- Saini N, Kaur S, Dhaliwal SS, Singh S (2021) Assessment of soil organic carbon stocks in relation to variation in physiography under sub-mountainous Shiwalik ranges of lower Himalayas, India. *Carbon Manag* 12:265–273. <https://doi.org/10.1080/17583004.2021.1910901>
- Sallam A, Steinbu A (2009) *Clostridium sulfidigenes* sp. nov., a mesophilic, proteolytic, thiosulfate- and sulfur-reducing bacterium isolated from pond sediment. *Int J Syst Evol Microbiol* 59:1661–1665. <https://doi.org/10.1099/ijls.0.004986-0>
- Sarker S, Hossain MMS, Rahman S, Sm C (2021) A review of bioturbation and sediment organic geochemistry in mangroves. *Geol J* 56:2439–2450. <https://doi.org/10.1002/gj.3808>
- Sewilam H, Kimera F, Nasr P (2023) Water energy food nexus model: an integrated aqua-agriculture system to produce tilapia and sweet basil using desalinated water. *Environ Sci Pollut Res* 30:15975–15990. <https://doi.org/10.1007/s11356-022-23240-0>
- Sherry A, Grant RJ, Aitken CM, Jones M, Bowler BF, Larter SR, Head IM, Gray ND (2020) Methanogenic crude oil-degrading microbial consortia are not universally abundant in anoxic environments. *Int Biodeterior Biodegrad* 155:105085. <https://doi.org/10.1016/j.ibiod.2020.105085>
- Sohaib M, Al-Barakah FN, Migdadi HM, Alyousif M, Ahmed I (2023) Ecological assessment of physico-chemical properties in mangrove environments along the Arabian Gulf and the Red Sea coasts of Saudi Arabia. *Egypt J Aquat Res* 49:9–16. <https://doi.org/10.1016/j.ejar.2022.11.002>
- Soltanpour PN (1991). Determination of nutrient availability and elemental toxicity by AB-DTPA soil test and ICPS. In *Advances in Soil Science: Volume 16* (pp. 165–190). New York, NY: Springer New York. [https://link.springer.com/chapter/10.1007/978-1-4612-3144-8\\_3](https://link.springer.com/chapter/10.1007/978-1-4612-3144-8_3)
- Sombrero A, Benito AD (2010) Carbon accumulation in soil. Ten-year study of conservation tillage and crop rotation in a semi-arid area of Castile-Leon, Spain. *Soil Tillage Res* 107(2):64–70. <https://doi.org/10.1016/j.still.2010.02.009>
- Suda K, Ikarashi M, Tamaki H, Tamazawa S (2021) Methanogenic crude oil degradation induced by an exogenous microbial community and nutrient injections. *J Pet Sci Eng* 201:108458. <https://doi.org/10.1016/j.petrol.2021.108458>
- Tan B, Ng C, Nshimiyimana JP, Loh LL, Gin KY, Thompson JR (2015) Next-generation sequencing (NGS) for assessment of microbial water quality: current progress, challenges, and future opportunities. *Front Microbiol* 6:1027. <https://doi.org/10.3389/fmicb.2015.01027>
- Tang H, Xiang G, Xiao W, Yang Z (2024) Microbial mediated remediation of heavy metals toxicity: mechanisms and future prospects. *Front Plant Sci* 15:1420408. <https://doi.org/10.3389/fpls.2024.1420408>
- Thai TD, Lim W, Na D (2023) Synthetic bacteria for the detection and bioremediation of heavy metals. *Front Bioeng Biotechnol* 11:1178680. <https://doi.org/10.3389/fbioe.2023.1178680>
- Thomson T, Ellis JJ, Fusi M, Prinz N, Bennett-Smith MF, Aylagas E, Carvalho S, Jones BH (2022) The right place at the right time: seasonal variation of bacterial communities in arid *Avicennia marina* soils in the Red Sea is specific to its position in the

- intertidal. *Front Ecol Evol* 10:845611. <https://doi.org/10.3389/fevo.2022.845611>
- Ukpong LE (2007) Vegetation and soil acidity of a mangrove swamp in southeastern Nigeria. *Soil Use Manage* 11(3):141–144. <https://doi.org/10.1111/j.1475-2743.1995.tb00512.x>
- Van Goethem MW, Makhalanyane TP, Cowan DA, Valverde A (2017) Cyanobacteria and alphaproteobacteria may facilitate cooperative interactions in niche communities. *Front Microbiol* 8:2099. <https://doi.org/10.3389/fmicb.2017.02099>
- Wainwright BJ, Millar T, Bowen L, Semon L, Hickman KJ, Lee JN, Yeo ZY, Zahn G (2023) The core mangrove microbiome reveals shared taxa potentially involved in nutrient cycling and promoting host survival. *Environ Microbiol* 18(1):47. <https://doi.org/10.1186/s40793-023-00499-5>
- Wang F, Xiao K, Santos IR, Lu Z, Tamborski J, Wang Y, Yan R, Chen N (2022) Porewater exchange drives nutrient cycling and export in a mangrove-salt marsh ecotone. *J Hydrol* 606:127401. <https://doi.org/10.1016/j.jhydrol.2021.127401>
- Wang G, Guan D, Peart MR, Chen Y, Peng Y (2013) Ecosystem carbon stocks of mangrove forest in Yingluo Bay, Guangdong Province of South China. *For Ecol Manage* 310:539–546. <https://doi.org/10.1016/j.foreco.2013.08.045>
- Wang Q, Wang C, Yu W, Turak A, Chen D, Huang Y, Ao J, Jiang Y, Huang Z (2018) Effects of nitrogen and phosphorus inputs on soil bacterial abundance, diversity, and community composition in Chinese for plantations. *Front Microbiol* 9:1–10. <https://doi.org/10.3389/fmicb.2018.01543>
- Wang Z, Li X, Zhang L, Wu J, Zhao S, Jiao T (2022) Effect of oregano oil and cobalt lactate on sheep in vitro digestibility, fermentation characteristics and rumen microbial community. *Animals* 12:118. <https://doi.org/10.3390/ani12010118>
- Wemheuer F, Taylor JA, Daniel R, Johnston E, Meinicke P, Thomas T, Wemheuer B (2020) Tax4Fun2: prediction of habitat-specific functional profiles and functional redundancy based on 16S rRNA gene sequences. *Environ Microbiomes* 15:1–12. <https://doi.org/10.1186/s40793-020-00358-7>
- Wu D, Xu Z, Min S, Wang J, Min J (2024) Characteristics of microbial community structure and influencing factors of Yangcheng Lake and rivers entering Yangcheng Lake during the wet season. *Environ Sci Pollut Res* 31:9565–9581. <https://doi.org/10.1007/s11356-023-31810-z>
- Yan L, Kuang Y, Xie X, Peng K, Deng Y, Gan Y, Li Q, Zhang Y (2024) Insights into nitrogen biogeochemical cycling in mangrove wetland from genome-resolved metagenomic sequencing. *J Hydrol* 640:131741. <https://doi.org/10.1016/j.jhydrol.2024.131741>
- Yang J, Gao J, Liu B, Zhang W (2014) Estuarine, coastal and shelf science sediment deposits and organic carbon sequestration along mangrove coasts of the Leizhou Peninsula, southern China. *Estuar Coast Shelf Sci* 136:3–10. <https://doi.org/10.1016/j.ecss.2013.11.020>
- Zhang R, Cheng Z, Zang C, Cui C, Zhang C, Jiao Y, Li F, Li X, Yang K, Luo Q (2023) Supplementation of 5, 6-dimethylbenzimidazole and cobalt in high-concentrate diet improves the ruminal vitamin B 12 synthesis and fermentation of sheep. *Fermentation* 9:956. <https://doi.org/10.3390/fermentation9110956>
- Zhang Y, Dong J, Yang B, Ling J, Wang Y, Zhang SI (2009) Bacterial community structure of mangrove sediments in relation to environmental variables accessed by 16S rRNA gene-denaturing gradient gel electrophoresis fingerprinting. *Sci Mar* 73:487–498. <https://doi.org/10.3989/scimar.2009.73n3487>

**Publisher's Note** Springer Nature remains neutral with regard to jurisdictional claims in published maps and institutional affiliations.